



**ASJP**  
Algerian Scientific Journal Platform



# Journal of Building Materials and Structures

---

VOL. 4 (2017)

---

An open access peer-reviewed journal  
ISSN 2353-0057



## Strength and durability of low-impact environmental self-compacting concrete incorporating waste marble powder

Boukhelkhal A<sup>1,\*</sup>, Azzouz L<sup>1</sup>, Benabed B<sup>1</sup>, Belaïdi ASE<sup>1</sup>

<sup>1</sup> Civil Engineering Laboratory, University of Laghouat, 03000, Algeria.

\* Corresponding Author: [a.boukhelkhal@lagh-univ.dz](mailto:a.boukhelkhal@lagh-univ.dz)

---

**Abstract.** This research studies the effect of waste marble powder (WMP) as substitute of Portland cement on strength and durability of self-compacting concrete (SCC) in order to produce SCC with reduced impact environmental. For this purpose, five mixtures were designed in which four mixtures contained WMP at substitution levels of 5, 10, 15, 20%, and mixture included only the Portland cement as control mix. The realized tests are compressive strength at 3, 7 and 28 days, water capillary absorption, water absorption by immersion and sulfate attack. The results show a reduction in the compressive strength with increasing WMP content. The use of WMP was found to increase both of the water capillary absorption and water absorption by immersion. SCC containing WMP subjected to magnesium sulfate attack presented a lower expansion and higher resistance to sulfate aggressions.

---

**Key words:** self-compacting concrete, waste marble, environment, strength, durability.

### Introduction

Self-compacting concrete (SCC), Self-consolidating concrete, self-leveling concrete, highly-flowable concrete or non-vibrating concrete are very fluid concretes that flow and compact under their proper weight without any effort of compaction or vibration even in highly reinforced structural elements or complex formwork (Naik et al, 2012; Kurita et Nomura, 1998). SCC was appeared and used for the first time in Japan three decades ago, its use was not stopped because SCC has special and interesting properties at fresh state such as flowability, passing ability and resistance to segregation. For achieving these contradictory properties, the formulation of SCC needs the use of high Portland cement content (450-600 kg/m<sup>3</sup>) and superplasticizer (SP). However, using high volume of Portland cement causes many problems such as:

- Increase in the consumption of cement
- Environmental impacts due to CO<sub>2</sub> emissions
- Consumption of energy and natural resources
- High production cost since the cement is the most expensive element in the concrete
- Risk of cracking associate to the high heat of cement hydration

In order to produce low-impact environmental, economic and durable SCC, the cement is replaced by fine additive materials (FAM) having large proportion of fine particles (<80 μm) such as slag, limestone, fly ash, rice husk ash...etc. The reuse of industrial by-products as FAM is a good solution to ensure the equilibrium of eco-system, biological components of the environment and public health (Sadek et al; 2016). Another solution consists in the incorporation of industrial waste materials as fine or coarse aggregates, which can contribute effectively to sustainable development. Using some types of FAM were shown to reduce the

dosage of SP compared to SCC with only Portland cement. The characteristics of SCC are strongly affected by the type, source, chemical, mineralogical, physical and mechanical properties of FAM. The incorporation of FAM in binary and ternary blended cement improves not only the fresh properties but also the hardened properties of SCC (Sonebi, 2004; Belaidi et al, 2015; Belaidi et al, 2012; Boukhelkhal et al, 2016; Safiuddin, 2008; Uysal et Yilmaz, 2011; Boukhelkhal, 2012; Boukhelkhal et al, 2012). Previous studies found that the use of FAM having different grain-size and morphology enhances the compactness and provides a better workability and cohesiveness by improving the grain-size distribution and particle packing. On other hand, this reduces the risk of cracking associated to the heat of hydration leading therefore to superior performance of SCC at long-term (Sonebi et Bartos, 1999; Boukendakdji et al, 2012). Recycling waste powders of marble and granite in the production of SCC was proved to be useful because the marble powder acts as filler, and granite powder acts as pozzolanic material despite its small pozzolanic activity (Sadek et al, 2016). Benabed et al (2016) have studied the effect of limestone powder as a partial replacement of crushed quarry sand on properties of self-compacting repair mortars, they concluded that the use of limestone powder at substitution rate of 10 to 15% is beneficial from rheological and strength properties. Research conducted by Chirici et al (2006), was demonstrated that including natural pozzolana (NP) in cement mortars increases the strength at later ages and enhances its resistance to acid and sulfate attacks and chloride ion penetration. Mortars with silica fume (SF), metakaolin (MK) and fly ash (FA) have shown an enhancement in compressive strength, dynamic modulus, ultrasonic pulse velocity, transport properties, sulfate resistance and freezing-thawing resistance (Aghabaglouet al, 2014). Pozzolanic fine additive materials such as SF, MK and FA are characterized by its high specific surface area and pozzolanic reaction in which additional calcium silicate hydrate CSH forms by reaction between reactive silica and calcium hydroxide produced by the cement hydration.

Marble stone is locally available in some quarries in the East of Algeria and is generally used in buildings for the preparation of slabs and tiles for decorative purposes. However, the process of cutting, shaping and lustrating of the marble stones generates a fine material know as waste marble powder which is not exploited and can pose a serious environmental problems. From this study, an attempt was conducted to produce a reduced impact environmental and durable SCC by exploiting the waste marble powder and investigating its effect as a fine additive materials on the strength and durability properties of SCC.

## **Experimental procedure**

### **2.1. Material properties**

The cement used in this study is an artificial Portland cement (CEMI) class 42.5. Waste marble powder subject of this study is a waste powder resulting from cutting, shaping and lustrating of the marble stones. The chemical composition and physical properties of WMP and cement are given in Table 1. From this table, the WMP is mainly consisted of lime (56.01%). As fine aggregate (FA), a river sand characterized by granular class of 0/5, and a continuous particles size distribution was used. For coarse aggregate (CA), two classes 3/8 and 8/15 were used. The physical properties of the aggregate are shown in Table 2. The superplasticizer used is a polycarboxylates based High-Range Water Reducers (HRWR). It has a specific gravity and pH of 1.07g/cm<sup>3</sup> and 8, respectively. Locally available potable water was used for mixing SCC constituents.

---

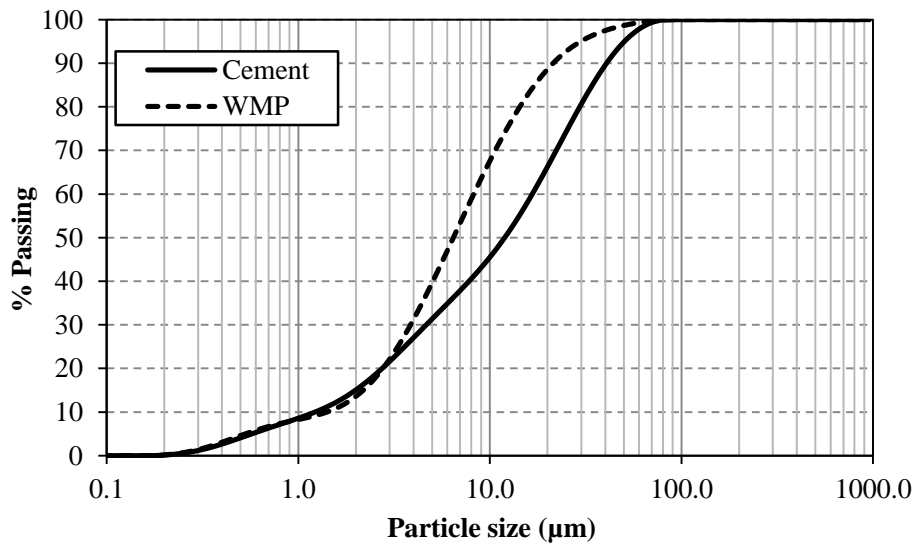
**Table 1. Chemical composition and physical properties of cement and waste marble powder.**

Component (%)	Cement	Waste marble powder
SiO <sub>2</sub>	20.14	0.42
CaO	63.47	56.01
MgO	2.12	0.12
Al <sub>2</sub> O <sub>3</sub>	3.71	0.13
Fe <sub>2</sub> O <sub>3</sub>	4.74	0.06
SO <sub>3</sub>	2.67	0.01
K <sub>2</sub> O	0.47	0.01
TiO <sub>2</sub>	0.21	0.01
Na <sub>2</sub> O	0.69	0.43
P <sub>2</sub> O <sub>5</sub>	0.06	0.03
Loss ignition	1.72	42.78
Density	3.1	2.7
Finesses (cm <sup>2</sup> /g)	3300	3600

**Table 2. Physical properties of aggregates.**

Aggregate	FA 0/5	CA 3/8	CA 8/15
Absorption Coefficient (%)	0.59	1.56	2.26
Density	2.60	2.61	2.54
Water content (%)	0.03	0.17	0.13

In order to determine particle size distribution of WMP and cement, laser distribution analysis was realized and the results are illustrated in Figure 1. The results indicate that WMP is relatively finer than the cement, and about 70% of particles of WMP have a diameter lower than 10  $\mu\text{m}$ .

**Fig 1. Particle size distribution of cement and waste marble powder.**

## 2.2. Mix design

Five mixtures were designed to study the effect of waste marble powder on the strength and durability of SCC. The binder content, water / binder ratio and dosage of superplasticizer were respectively equal to 470Kg/m<sup>3</sup>, 0.4 and 0.9%. The control mixture contains only the Portland cement as binder, while other mixtures include the WMP at different substitution levels 5, 10, 15 and 20 %. The mix proportions of different mixtures are presented in Table 3.

**Table 3. Mix proportions of SCC.**

Materials	Mixes				
	0WMP	5WMP	10WMP	15WMP	20WMP
Cement (kg)	470	446.5	423	399.5	376
WMP (%)	0	5	10	15	20
WMP (kg)	0	23.5	47	70.5	94
Sand 0/5 (kg)	882.9				
Gravel 8/15 (kg)	553				
Gravel 3/8 (kg)	277				
Water (kg)	188				
Superplasticizer (kg)	4.23				
w/b	0.4				

### 2.3. Test protocol

#### 2.3.1. Compressive strength

Compressive strength measurements of each mixture were made on six pieces of three prismatic specimens of 70×70×280 mm size that were previously crushed by flexion. The test was carried out using a hydraulic press with a capacity of 2000kN at concrete age of 3, 7 and 28 days according to the European Standard (EN 12390-3, 2001).

#### 2.3.2. Water capillarity Absorption

Water capillary absorption was evaluated on concrete prismatic specimens of 70×70×280 mm size after initial water-curing of 28 days according to the French standards (NF P 18-502, 1989). The concrete specimens were firstly dried at 105 ± 5 °C for 72 hours before being sealed by waterproof material on the sides to ensure one direction of water flow, and stored in water on their cross section with a constant water height of 5 mm. The increase in specimen mass was measured regularly every 5 minutes until 90 minutes. The mass of water absorbed per unit area was plotted against the square root of time. The coefficient of water capillary absorption  $C_c$  is determined using the following equation:

$$\frac{\Delta M}{A} = C_c \sqrt{t} \quad (1)$$

Where  $\Delta M$ : mass of water absorbed at time  $t$  (g),  $A$ : exposed area of the specimen (cm<sup>2</sup>),  $t$ : elapsed time (min),  $C_c$ : coefficient of water capillary absorption (g/cm<sup>2</sup>/min<sup>0.5</sup>).

#### 2.3.3. Water Absorption by immersion

In this test, three concrete prismatic specimens of 70×70×280 mm size from each mixture were cured in water for 28 days and dried after that at 105 ± 5 °C for 72 hours. The specimens were weighed  $M_0$  and immediately immersed in water at approximately 21 °C for not less than 48 hours before being weighed in accordance with ASTM C642-97 (1997). The coefficient of water absorption by immersion  $A_i$  is given by the following equation:

$$A_i = \left( \frac{M_s - M_d}{M_d} \right) \times 100 \quad (2)$$

Where  $M_s$ : saturated mass (g),  $M_d$ : dried mass (g),  $A_i$ : coefficient of water absorption by immersion (%).

### 2.3.4 . Sulfate attack

The sulfate exposure testing procedure was conducted by immersing mortar specimens in sulfate solution after an initial water-curing period of 28 days. 25×25×285 mm prism and 50×50×50 mm cube specimens were prepared for sulfate resistance tests. The specimens were immersed in 5% magnesium sulfate solution at 23±2 °C according to ASTM C1012-04 (2004). The solution was renewed every 4 weeks to minimize the increase of pH due to the leaching OH<sup>-</sup> ions from the mortar specimen. The length changes of prism specimens were measured weekly for the first four months and monthly until six months, for cube specimens, the compressive strength was determined at 0, 28, 56, 90 and 180 days. The strength gain or loss of the mortar cube specimens was investigated by comparing the strength before immersion (0 days) and after immersion (28, 56, 90 and 180) in sulfate solution. Visual control was performed on selected specimens.

## 3. Results and discussion

### 3.1. Compressive strength

Figure 2 shows the evolution of compressive strength with age of testing. The compressive strength of all hardened SCC mixtures increases progressively with curing age. Due to its high volume in Portland cement, the control mix has for all ages the highest values of strength. With the same amount of the binder, the substitution of the cement by the WMP decreases the strength of SCC. The compressive strength of 0WMP; 5WMP; 10WMP; 15WMP and 20WMP mixes at 28 days are 37.2; 36.7; 34.5; 28.8 and 26.1 MPa, respectively. SCC with 5% of WMP has developed a similar compressive strength with SCC control at 28 days (37 MPa) in comparison with the reference mixture, the compressive strength of 5WMP; 10WMP; 15WMP and 20WMP mixture decreased by 1.3; 7.3; 22.6; 30 and 36.6% at 28 days.

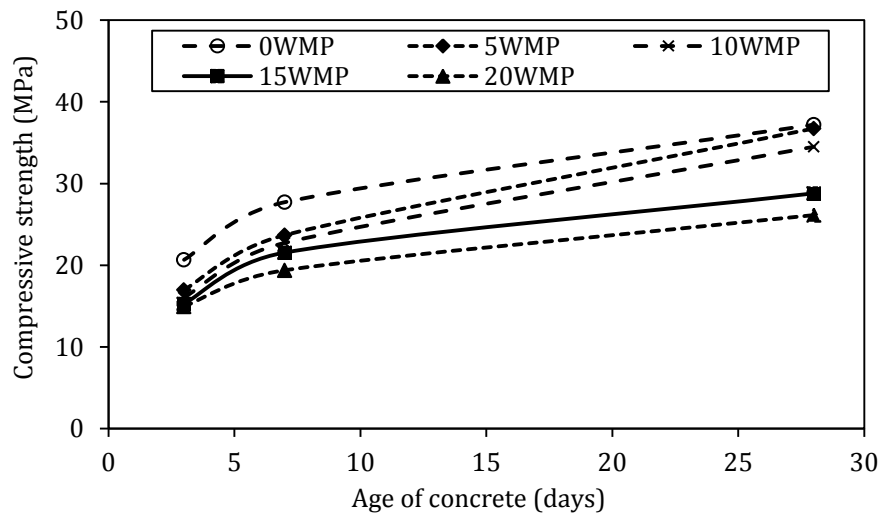


Fig 2. Evolution of compressive strength.

These results are in accordance with those reported by other researchers (Güneyisi et al, 2009; Bouziani et al, 2011). The decrease in compressive strength could be due to the use of a fine inert material having a fineness approximation similar to that of the Portland cement (low filling effect), and to the reduction in the water/cement ratio by adding WMP. In addition, with introducing WMP, the cement paste was insufficient to coat all the sand particles, which consequently leads to a decrease in compressive strength (Benabed et al, 2016). Mixture containing 20% of WMP and a cement content of about 380 kg/m<sup>3</sup> had developed at 28 days a

similar compressive strength with ordinary concrete that is generally used in ordinary constructions (26MPa). The replacement of cement and sand by marble powder (MP) at substitution rate of 10% decreases the compressive strength of mortars, and mortars with MP substituted by sand performed better than mortar with MP substituted by cement (Corinaldesi et al, 2010)

### 3.2. Water capillary Absorption

The influence of WMP on the water capillary absorption is presented in Figure 3. The obtained values show an increase in the water absorption with time for all mixtures. The increase in WMP content increases the water absorption. It should be noted that the reference mixture has the lowest water absorption value, while the water absorption value of mix including 20% of WMP is the highest. The coefficient of water capillary absorption ( $C_c$ ) of 0WMP; 5WMP; 10WMP; 15WMP and 20WMP mixes are  $3.3 \times 10^{-2}$ ;  $3.6 \times 10^{-2}$ ;  $3.7 \times 10^{-2}$ ;  $3.9 \times 10^{-2}$  and  $4 \times 10^{-2}$  g/mm<sup>2</sup>/min<sup>0.5</sup>. The values demonstrated that increasing WMP content from 5 to 20% leads to an increase in the coefficient of water capillary absorption from 9.7 to 22.6%. Similar results were obtained in concrete containing slag at substitution levels of 15, 30 and 50%, with w/b ratio of 0.65, tested at 28 days (Hadjsadoka et al, 2012).

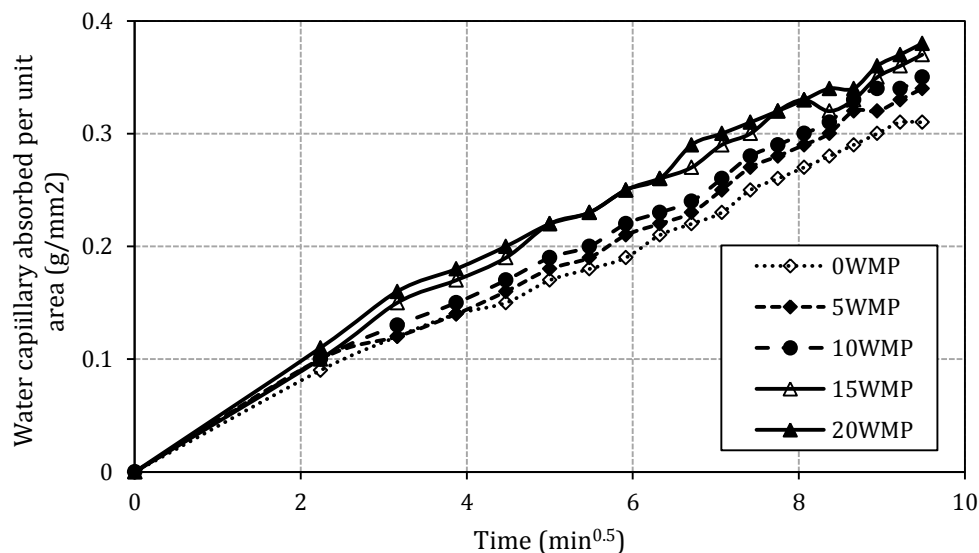


Fig 3. Effect of waste marble powder on water capillary absorption.

### 3.3. Water Absorption by immersion

The durability of concretes is significantly influenced by their pore structure. This parameter can be evaluated by measuring water Absorption by immersion. The variation of water absorption by immersion for all SCC mixes is illustrated in Figure 4. It is clear from the obtained results that the increase in the amount of substituted WMP leads to an increase in the water absorption. The water absorption values of mixtures containing 0, 5, 10, 15 and 20% of WMP are 4.67; 5.10; 5.11; 5.13 and 5.17%, respectively. This means that incorporation of WMP at substitution levels of 5, 10, 15 and 20% increases the water absorption rate by 9.26, 9.47, 9.9 and 10.9%, respectively. It was noted that all tested SCC have low water absorption (less than 10%) (Siddique, 2013), exception for mix that including 20% of WMP. In other hand, the obtained water absorption values are superiors to those found in mortar mixtures incorporated fly ash, silica fume and metakaolin (1.8 to 4.2%). These may be attributed to the use of inert material that having a low

filling effect because both the cement and WMP have approximately similar fineness (Aghabaglouet al, 2014). Similar effects was observed in SCC made bottom ash in which increasing the amount of bottom ash increases water absorption by immersion (Siddique, 2013).

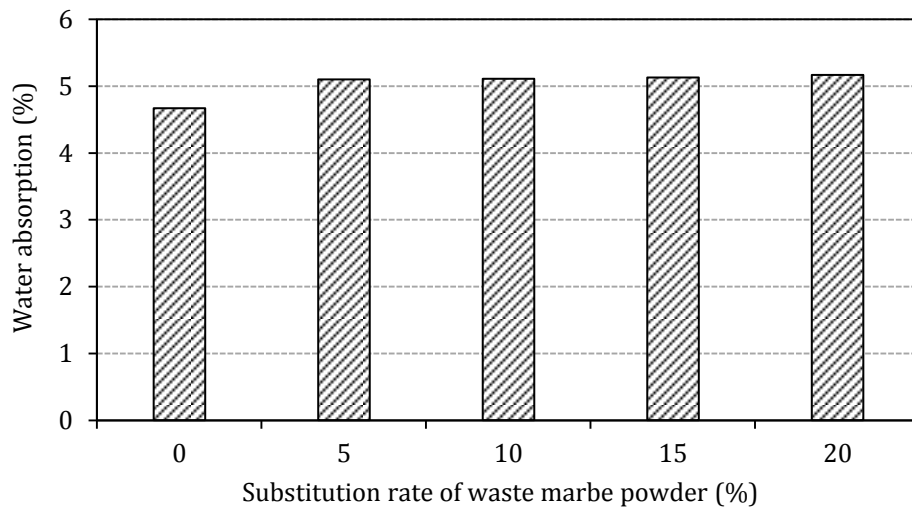


Fig 4. Variation of water absorption versus the substitution rate of waste marble powder.

### 3.4. Correlation between compressive strength and water absorption by immersion

Correlation between compressive strength and water absorption by immersion is illustrated in figure 5. Compressive strength decreases with increasing water absorption by immersion. It can be noted that there is a moderate linear relationship between these parameters. The coefficient of correlation was equal to 0.37. This relation suggests that with the increase in water absorption by immersion, SCC is expected to have reduced compressive strength.

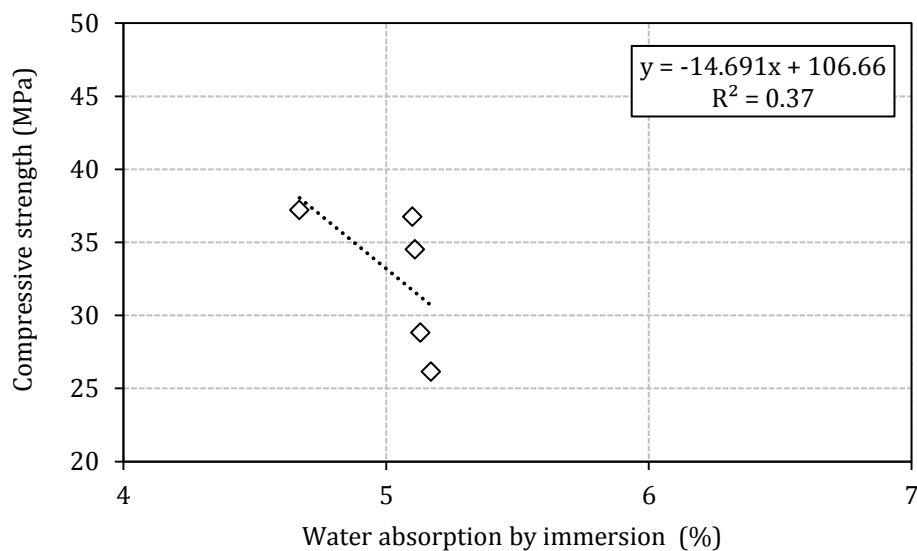


Fig 5. Correlation between compressive strength at 28 days and water absorption by immersion.

### 3.5. Correlation between compressive strength and water capillary absorption

Figure 6 presents the correlation between compressive strength at 28 days and coefficient of water capillary absorption of various SCC mixtures. It is clear from the obtained results that the decrease in compressive strength is associated to the decrease of the water capillary absorption



coefficient. The results indicate that there is an excellent relationship between these parameters. The coefficient of correlation was found to be close to 1.

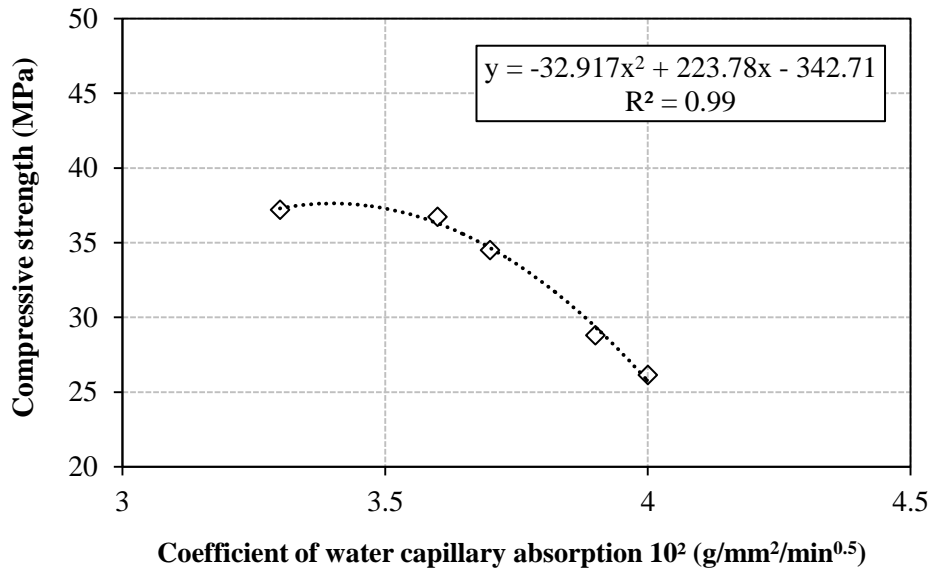


Fig 6. Correlation between compressive strength at 28 days and coefficient of water capillary absorption.

### 3.6. Effects of sulfate attack

#### 3.6.1. Expansion

Figure 7 depicts the evolution of the expansion of mortars with and without WMP. The expansion increases with increase of the immersion period in sulfate solution. It had been observed that there is an inversely proportional relation between the increase in WMP volume and the decrease in the expansion.

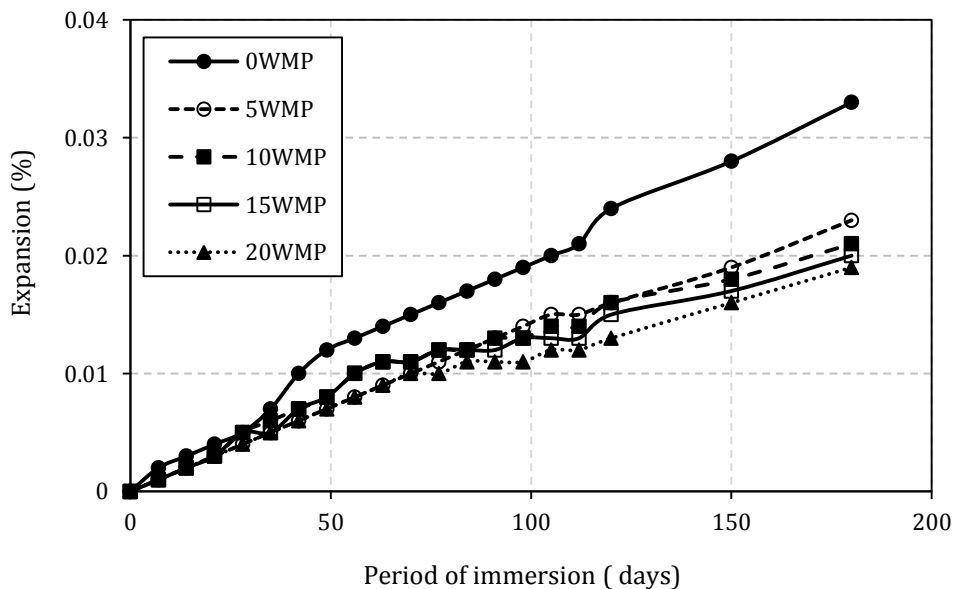


Fig 7. Evolution of the expansion of mortar specimens immersed in magnesium sulfate solution.

The results showed that the mix without WMP has the highest values of expansion, whereas the mix with 20% of WMP showed the lowest values of expansion. At 180 days, the expansion values of 0WMP, 5WMP, 10WMP, 15WMP and 20WMP mixes are  $3.3 \times 10^{-2}$ ,  $2.3 \times 10^{-2}$ ,  $2.1 \times 10^{-2}$ ,  $2 \times 10^{-2}$  and

$1.9 \times 10^{-20}$ . This means that the incorporation of WMP at substitution rate of 5, 10, 15 and 20% decreased the expansion by 30, 36, 39 and 42%, respectively. The increase in the expansion for all mixes is attributed to the formation of two voluminous products (gypsum and ettringite). The decrease in the expansion for mortars with WMP compared to mortar with plain cement is due to the reduction in the cement content which reduces the  $C_3A$  content in the binder and the volume of the ettringite product (Aghabaglou et al, 2014).

### 3.6.2. Compressive strength

Figure 8 presents the evolution of the compressive strength of mixtures with and without WMP as a function to the period of immersion in magnesium sulfate solution. It can be seen from this figure that the reference mix shows a strength gain of about 24% at immersion period of 28 days. However, after this period the strength gain slightly decreases at immersion period of 56 and 90 days (18 and 17%), but considerably decreases at 180 days (1%). For mixes containing WMP, the strength gain increases until 180 days. The strength gain of 5WMP, 10WMP, 15WMP and 20WMP mixes is about 13, 26, 28 and 21% for immersion period of 28, 56, 90 and 180 days, respectively. This demonstrates that the inclusion of 10% of WMP by partial replacement of the cement is considered the optimum substitution rate. The strength gain might be attributed to the continuous hydration of anhydrated cement products and the reaction of  $MgSO_4$  with  $Ca(OH)_2$  to form two voluminous elements (gypsum and ettringite) which fill in the micro-pores leading to a denser structure. The reduction in strength gain is due to the expansion effect of the sulfate attack which leads to the formation of micro-cracks and softening of the cement matrix (Ghrici et al, 2006).

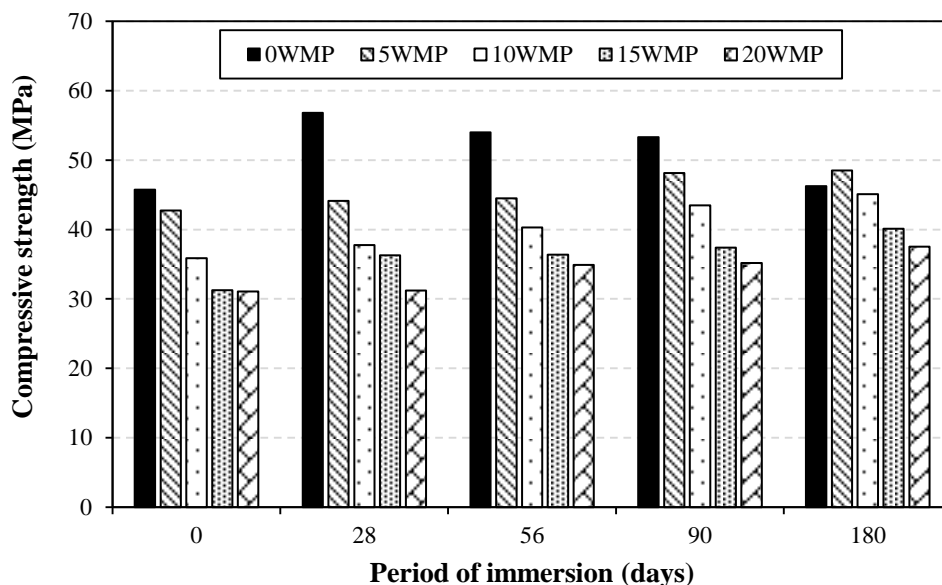


Fig 8. Evolution of compressive strength of mortar specimens immersed in magnesium sulfate solution.

### 3.6.3. Visual control

Visual inspection on some selecting mortar specimens was carried out after 180 days of immersion in the magnesium sulfate solution to evaluate the visible signs of softening, cracking and spalling in the mortar specimens, the results are shown in Figure 9. From this control, a low spalling deterioration was observed especially at the edges and corners of some specimens, in particular those of the control mortar. This is due to the fact that these places are exposed to two (edges) or three (corners) penetration flux of sulfate ions, which accelerates their degradation.



Fig 9. Visual control of mortar specimens.

#### 4. Conclusions

This investigation was conducted to assess the strength and durability of reduced environmental impact SCC made with waste marble powder. From the obtained results in this investigation, the following conclusions can be drawn:

- SCC made with waste marble powder at replacement level of 5% developed approximately similar compressive strength with control SCC. At 28 days, compressive strength values ranging from 26 to 37 MPa were obtained. These results allow the use of different replacement levels of WMP for different concrete purposes. For example, SCC containing WMP content of 10% can be used in a structure when the desired strength is about 35MPa.
- Concerning the water capillary absorption and water absorption by immersion, a slight increase in amount of water absorbed was observed when the cement is partially replaced by WMP.
- Correlations between compressive strength at 28 days and water absorption properties were found very good with a coefficient of correlation more than 0.9.
- Incorporating WMP in SCC mixes immersed in magnesium sulfate solution was found to decrease the expansion and to improve the resistance to sulfate aggressions.
- Finally, it can be concluded that the exploitation of waste marble powder as fine materials in production of SCC is very advantageous from technical, economical and environmental points of view.

#### 5. References

- Aghabaglou AM, Sezer GI, Ramyar K. (2014). Comparison of fly ash, silica fume and metakaolin from mechanical properties and durability performance of mortar mixtures view point. *Construction and Building Materials*, 70, 17-25.
- ASTM C 642-97. (1997). Standard test method for density, absorption, and voids in hardened concrete. American Society for Testing and Materials, USA.
- ASTM C 1012-04. (2004). Standard test method for length change of hydraulic cement mortar exposed to a sulfate solution. American Society for Testing and Materials, USA.
- Belaidi ASE, Kenai S, Kadri EH, Soualhi H, Benabed B. (2015). Effects of experimental ternary cements on fresh and hardened properties of self-compacting concretes. *Journal of Adhesion Science and Technology*, 30, 247-261.
- Belaidi ASE, Azzouz L, Kadri E, Kenai S. (2012). Effect of natural pozzolana and marble powder on the properties of self-compacting concrete. *Construction and Building Materials*, 31, 251-257.
- Boukhelkhal A, Azzouz L, Belaïdi ASE, Benabed B. (2016). Effects of marble powder as a partial replacement of cement on some engineering properties of self compacting concrete. *Journal of Adhesion Science and Technology*, 30(22), 2405-2419.
- Boukhelkhal A. (2012). Rheology, physical and mechanical characterization and durability of self-compacting concrete made with marble powder. [MSc thesis]. University of Laghouat, Algeria. p.170.

- 
- Boukhelkhal A, Azzouz L, Belaïdi ASE, Benabed B. (2012). Effect of marble powder on the properties of self-compacting concrete at fresh state. In: Proceeding of First International international conference on civil engineering, Laghouat, Algeria.
- Boukendakdji O, Kadri EH, Kenai S. (2012). Effects of granulated blast furnace slag and superplasticizer type on the fresh properties and compressive strength of self-compacting concrete. *Cement and Concrete Composites*, 34(4), 583–590.
- Benabed B, Soualhi H, Belaidi ASE, Azzouz L, Kadri E, Kenai S. (2016). Effect of limestone powder as a partial replacement of crushed quarry sand on properties of self-compacting repair mortars. *Journal of Building Materials and Structures*, 3,15-30.
- Bouziani T, Benmounah A, Bederina M, Lamara M. (2011). Effect of marble powder on the properties of self-compacting sand concrete. *The Open Construction & Building Technology Journal*, 5, 25-29.
- Corinaldesi V, Moriconia G, R. Naik T. (2010). Characterization of marble powder for its use in mortar and concrete. *Construction and Building Materials*, 24(1), 113-117.
- EN 12390-3. (2001). Testing hardened concrete - Part 3: Compressive strength of test specimens. European committee for standardization, Bruxelles.
- Ghrici M, Kenai S, Meziane E. (2006). Mechanical and durability properties of cement mortar with Algerian natural pozzolana. *Materials Science*, 41(21), 6965–6972.
- Güneyisi E, Gesoğlu M, Özbay E. (2009). Effects of marble powder and slag on the properties of self-compacting mortars. *Materials and Structures*, 42, 813-826.
- Hadjsadoka A, Kenai S, Courard L, Michel F, Khatib J. (2012). Durability of mortar and concretes containing slag with low hydraulic activity. *Cement and Concrete Composites*, 34(5), 671–7.
- Kurita M, Nomura T. (1998). High-flowable steel fiber-reinforced concrete containing fly ash. In: Malhotra VM, editor. *Proceedings, sixth CANMET/ACI international conference on fly ash, silica fume, slag, and natural Pozzolans in concrete, SP-178*. Farmington Hills, MI: American Concrete Institute. p. 159–179.
- Naik R.T, Kumara R, W. Rammeh B, Canpolatc F. (2012). Development of high-strength, economical self-consolidating concrete. *Construction and Building Materials*, 30, 463-469.
- NF P 18-502 (1989). Water capillary absorption. Paris: AFNOR.
- Sadek DM, El-Attar MM, Haitham AA. (2016). Reusing of marble and granite powders in self-compacting concrete for sustainable development. *Cleaner Production*, 121, 19-32.
- Sonebi M. (2004). Medium strength self-compacting concrete containing fly ash: modeling using factorial experimental plans. *Cement and Concrete Research*, 34(7), 1199–1208.
- Safiuddin M. Development of self-consolidating high performance concrete incorporating rice husk ash. (2008). Phd thesis, University of Waterloo, Canada, p.359
- Sonebi M, Bartos PJ. (1999, September). Hardened SCC and its bond with reinforcement. In: *Proceeding of First International RILEM Symposium on Self-Compacting Concrete (PRO 7)*, Stockholm, Sweden.
- Siddique R. (2013). Compressive strength, water absorption, sorptivity, abrasion resistance and permeability of self-compacting concrete containing coal bottom ash. *Construction and Building Materials*, 47, 1444-1450.
- Uysal M, Yilmaz K. Effect of mineral admixtures on properties of self-compacting concrete. (2011). *Cement and Concrete Composites*, 33, 771–776.
-

## Recycling of rubber waste in sand concrete

Guendouz M <sup>1,\*</sup>, Boukhelkhal Dj <sup>2</sup>

1\* LME Laboratory, University of Medea, Medea, Algeria.

2 Geomaterials Laboratory, University of Blida, Blida, Algeria.

\* Corresponding Author: [guen12moh@gmail.com](mailto:guen12moh@gmail.com)

---

**Abstract.** The large development in the consumption of rubber is observed in the recent years, which leads to an increase of the production of rubber related waste. Rubbers are not hazardous waste, but they constitute a hazard for both environment and health, in case of fire in storage sites. So, recycling appears as one of the best solutions for disposing of rubber waste. This paper presents an experimental investigation dealing with the valorisation of rubber waste, specifically rubber obtained from old shoes sole waste. The waste rubbers are used form (0/5 mm) to mixes as addition at percentage (10%, 20%, 30% and 40%) in sand concrete. The physical (workability, bulk density), mechanical (compressive and flexural strength) and thermal properties are studied and analysed. The results indicate that the incorporation of rubber waste particles in sand concrete contributes to increase the workability and reduce the bulk density of all studied sand concrete. The obtained results show that mechanical performance (compressive and flexural strength) decreases when the rubber content increases. Nevertheless, the presence of rubber aggregate leads to a significant reduction in thermal conductivity, which improves the thermal insulation performances of sand concrete. This study insures that reusing of recycled rubber waste in sand concrete gives a positive approach to reduce the cost of materials and solve some environmental problems.

---

**Key words:** Rubber; recycling; sand concrete.

### 1. Introduction

The fraction of rubber waste in household wastes is large and increases with time. In each country the waste composition is different, since it is affected by socioeconomic characteristics, consumption patterns and waste management programs, but generally the level of rubber in waste composition is high. The large volume of materials required for construction is potentially a major area for the reuse of waste materials. Recycling in concrete has advantages since it is widely used and has a long service life, which means that the waste is being removed from the waste stream for a long period. Many authors have reported the properties of concrete with used tyre rubbers. Their results indicate that the size, proportion, and surface texture of rubber particles affect the strength of used tyre rubber contained in concrete (Khatib et al., 1999; Fedroff et al., 1996; Eldin and Senouci, 1993; Ali et al., 2000; Rostami et al., 2000; Topcu, 1995; Fattuhi and Clark, 1996; Naik and Singh, 1991; Siddique and Naik, 2004; Lee et al., 1998; Goulias and Ali, 1998). Eldin et al (1993) conducted experiments to examine the strength and toughness properties of rubberised concrete mixtures. They used two types of tyre rubber, with different tyre rubber content. Their results indicated approximately 85% reduction in compressive strength, whereas the splitting tensile strength reduced by about 50% when the coarse aggregate was fully replaced by chipped tyre rubber. A smaller reduction in compressive strength (65%) was observed when sand was fully replaced by fine crumb rubber. Concrete containing rubber did not exhibit brittle failure under compression or splitting tension and had the ability to absorb a large amount of energy under compressive and tensile loads. A more in-depth analysis of their results indicates that an optimised mixture proportion is needed to optimise the tyre rubber content in the mixture. In recent years, used tyre chipped rubber

containing Portland cement concrete for uses in sound/crash barriers, retaining structures, and pavement structures has been extensively studied (Khatib et al., 1999; Eldin and Senouci, 1993; Ali et al., 2000). Test results showed that the introduction of used tyre chipped rubber considerably increases toughness, impact resistance, and plastic deformation but in almost all cases a considerable decrease in strength was observed. Khatib et al (1999) studied the influence of adding two kinds of rubber, crumb (very fine to be replaced for sand) and chipped (at the size of 10–50 mm to be replaced for gravel). They made three groups of concrete mixtures. In group A, crumb rubber to replace fines, in group B, chipped rubber to replace coarse aggregate, and in group C both types of rubber were used in equal volumes. In all, the three groups had eight different rubber contents in the range of 5–100% were used. They found that the compressive strength of concrete would decrease with increasing rubber content. For example, replacing 100% gravels by chipped rubber would decrease the compressive strength of concrete up to 90%. Meanwhile, they showed that the rubberised concrete made with chipped rubber has less strength than concrete made with crumb rubber.

This work focuses on the possibility of recycling rubber waste of shoes without any prior treatment as a partial replacement of natural aggregate in sand concrete, in order to minimize the cost of the final material. The influence of the proportion of rubber waste used on properties of the new material has been studied and analyzed.

## 2. Experimental program

### 2.1. Materials

The sand used was a dune sand available in south of Algeria, near the city of Tamanrasset. The particle size distributions of the used sand are shown in Figure 1 and the physical characteristics are presented in Table 1.

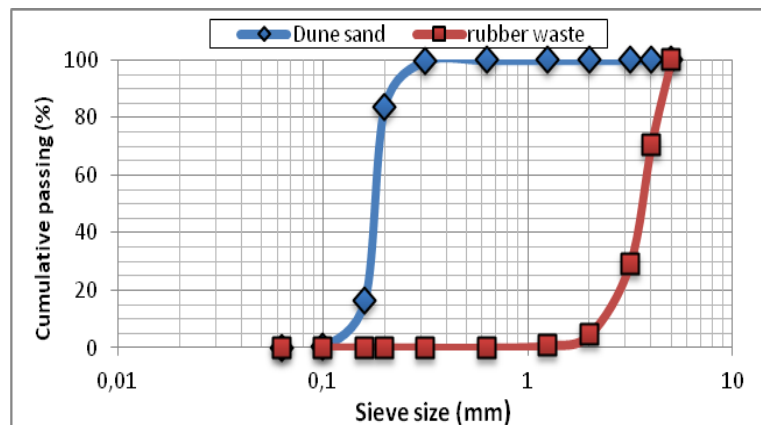


Fig 1. Particle size distribution of sand and rubber waste used.

Table 1. Physical properties of used sand.

Properties	Sand	Standard
Bulk density ( $\text{kg/m}^3$ )	1400	NP EN 1097-3
Specific density ( $\text{kg/m}^3$ )	2560	NP EN 1097-6
Water absorption (%)	2.66	NP EN 1097-6
Sand equivalent (%)	80.50	NP EN 933-8
Fineness modulus	0.84	NP EN 933-1
Compactness (%)	0.55	NF P 18-555
Porosity (%)	0.45	NF P 18-555
Thermal conductivity (W/m K)	1.3-1.4	NF EN ISO 8894-1

An industrial Portland cement CPJ-CEM II/A of class 42.5 is used. The physical characteristics are the following: specific density 3100 kg/m<sup>3</sup> and specific surface area 308 m<sup>2</sup>/kg, was used for all sand concrete mixtures.

The use of fillers in sand concrete composition is essential (AFNOR 1994). Their use is intended to complete the grading curve of sand in its finest part in order to obtain more compact concrete and reduce the cement content and therefore the cost of concrete. In this work the fillers used are the limestone powder. Their specific density is 2660 kg/m<sup>3</sup>, and specific surface area 242 m<sup>2</sup>/kg.

The rubber waste used in this work were obtained by the recycling the waste of shoes (Figure 2) discharged into the nature after were collected, are washed, compressed, crushed and extruded in the form of grains, and added in the mass of sand concrete with percentage (10%, 20%, 30% and 40%). The sieve analysis results are given in Figure 1, and the Table 2 lists the set of physical and thermal properties.



Fig 2. Particle size distribution of sand and rubber waste used.

Table 2. Physical and thermal properties of used rubber waste.

Properties	Rubber waste	Standard
Bulk density (kg/m <sup>3</sup> )	1500	NP EN 1097-3
Specific density (kg/m <sup>3</sup> )	800	NP EN 1097-6
Water absorption (%)	1.28	NP EN 1097-6
Fineness modulus	3.2	NP EN 933-1
Compactness (%)	53	NF P 18-555
Porosity (%)	47	NF P 18-555
Thermal conductivity (W/m K)	0.15	NF EN ISO 8894-1

A polycarboxylate plasticizer (Medafluid 104) produced by GRANITEX group (Algeria) with solid contents of 35% was used for all mixes. The mixing water used for the different mixes is the drinking water, free of impurities with a PH equal to 7.

## 2.2. Mix design

In this work, the optimal compositions of the sand concrete studied, without rubber waste, is based on the experimental method of project of Sablocrete (SABLOCRETE 1994). This gave for cement proportioning of 350 kg/m<sup>3</sup>, 1200 kg/m<sup>3</sup> of sand, 250 kg/m<sup>3</sup> of fillers, and a water/cement ratio of 0.85, a percentage of plasticiser of 1% of weight of cement. The rubber waste is added in sand concrete at dosages (0%, 10%, 20%, 30% and 40%). Literary codes identify each mixture in a precise way:

- **CSC**: Control sand concrete (without rubber).
- **SCRW**: Sand concrete with rubber waste.

All specimens were produced in laboratory environment with 20°C and 50% RH. After 24 h, they were removed from the molds and placed in water at 20°C and 100% relative humidity until the day of testing. This procedure was respected for all compositions and all tests.

### 2.3. Test procedure

The workability of concrete was measured in terms of slump according to NF P 18-451. The flexural strength was measured on 40×40 ×160 mm specimens at the ages of 28 days by a three-point bending test, using a testing machine according to EN 196-1. The half-samples resulting from this test were then submitted to compression test. The measurements of thermal conductivity led to the determination of the following parameters: thermal conductivity ( $\lambda$ ), on three 40×80×160 mm samples using a CT-Meter machine.

## 3. Results and discussion

### 3.1. Workability

The slump of sand concrete as a function the content of rubber waste is showed in Figure 3. The use of rubber waste as addition in sand concrete contributes to increase the slump of sand concrete, probably due to the presence of more free water in the mixes containing rubber than in the concrete mix containing natural aggregate since, unlike natural aggregate, rubber aggregate has a lower absorption coefficient than dune sand, which is in concordance with the results of Guendouz et al (2016). Khatib et al (1999) investigated the workability of rubcrete and reported that there is a decrease in slump with increase in rubber content as a percentage of total aggregate volume. They further noted that at rubber contents of 40%, slump was almost zero and concrete was not workable manually. It was also observed that mixtures made with fine crumb rubber were more workable than those with coarse tire chips or a combination of tire chips and crumb rubber. Siddique and Naik (2004) have reported that mortars incorporating rubber shreds achieved workability comparable to or better than a control mortar without rubber particles It was also observed that mixtures made with fine crumb rubber were more workable than those with coarse tire chips or a combination of tire chips and crumb rubber.

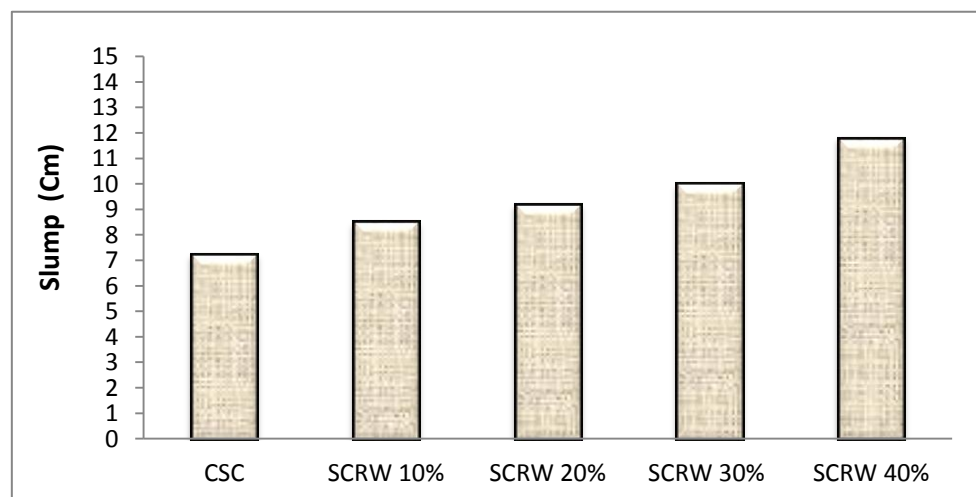


Fig.3. Slump of sand concrete as function of rubber waste content.

### 3.2. Bulk density

According to the results presented in Figure 4, the use of rubber waste as addition in sand concrete contributes to reduce the bulk density, probably due to the lower density of the rubber compared with the dune sand, which is in concordance with the results of Guendouz et al (2015). Khatib et al (1999) concluded that because of low specific gravity of rubber particles, unit weight of mixtures containing rubber decreases with the increase in the percentage of rubber content. Moreover, increase in rubber content increases the air content, which in turn



reduces the unit weight of the mixtures. The decrease in unit weight of rubcrete is found to be negligible when rubber content is lower than 10–20% of the total aggregate volume.

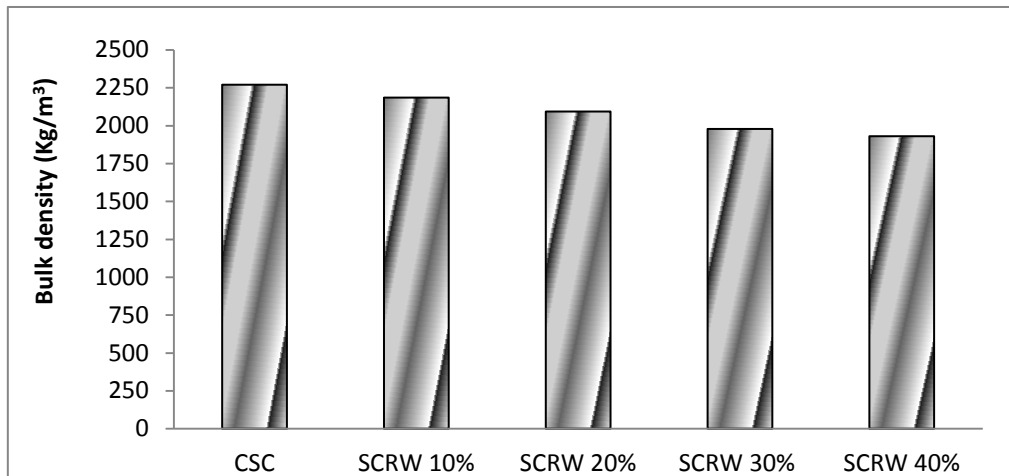


Fig.4. Bulk density of sand concrete as function of rubber waste content.

### 3.3. Mechanicals strength

The results of compressive and flexural strength of different sand concretes at 28 days of age are presented in Figure 5 and 6 respectively. The results displayed in Figure 5 and 6 show that compressive strengths of sand concrete decrease 15.7 % respectively for addition of 40% natural dune sand by rubber waste. Event thing in the case of the flexural strengths, which indicates that the addition of 40 % of the rubber waste in a sand concrete represents decrease the performances of new materials. This trend may be related to a poor adhesion between the surface of the rubber aggregate and binder paste which is likely to have contributed to such a strong decay of mechanical properties. Eldin and Senouci (1993) compared the use of rubber as coarse aggregates and the use of rubber chips as sand. The reductions of up to 85% of the compressive strength were observed when the coarse aggregate was replaced by rubber. A smaller reduction in compressive strength (65%) was observed when sand was replaced by crumb rubber. It was further observed that rubber-containing concrete did not exhibit brittle failure under compression. The strength reduction can be attributed both to a reduction of the quantity of the solid load-carrying material and to stress concentrations (tensile and compressive) in the paste at the boundaries of the rubber aggregate.

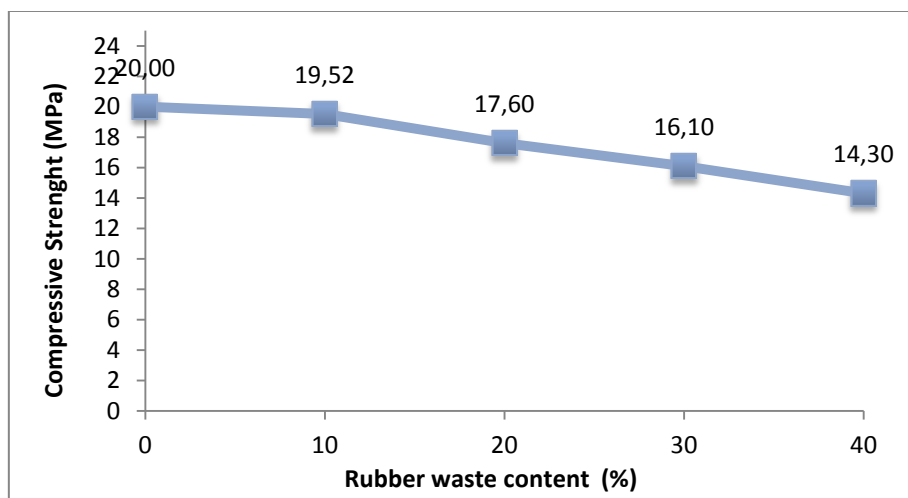


Fig.5. Compressive strength of sand concrete as function of rubber waste content.

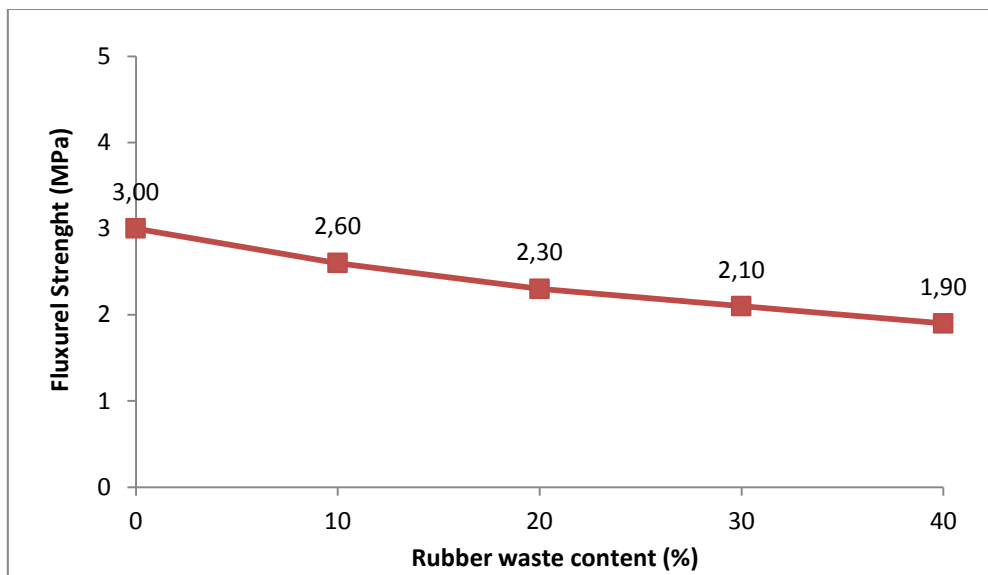


Fig.6. Flexural strength of sand concrete as function of rubber waste content.

### 3.4. Thermal Conductivity

Figure 7 give the thermal conductivity values of the specimens measured at 28 days. The thermal conductivity value of control sand concrete was 1.58 W/m K. This value decreased to 1.02 W/m K for dune SC when the replacement of rubber wastes into mixture with normal aggregate at a ratio of 40%. Rubber waste aggregate addition into SC composites caused the reduction in the values of TC of the specimens. It is thought that, this situation caused by the lower thermal conductivity value of the rubber (0.15 W/m K) than natural aggregate (2 W/m K) Lucolano et al (2013). So the decreasing thermal conductivity came also from the increase in porosity induced by the rubber waste. In fact the pores contain air which has a thermal conductivity value (0.024 W/mK) much lower than all the other components of the SC. Similar results were observed by several authors in composite systems, for example Hannawi et al. (2010) in a study on PF and PET in mortar composites, and it's showed a decreased in value of thermal conductivity of mortar containing PET about 50% lower than a traditional mortar. Akçaözog̃lu et al.(2013) find that the PET aggregate replacement with natural aggregate in mixture caused a reduction in the values of thermal conductivity value of the specimens.

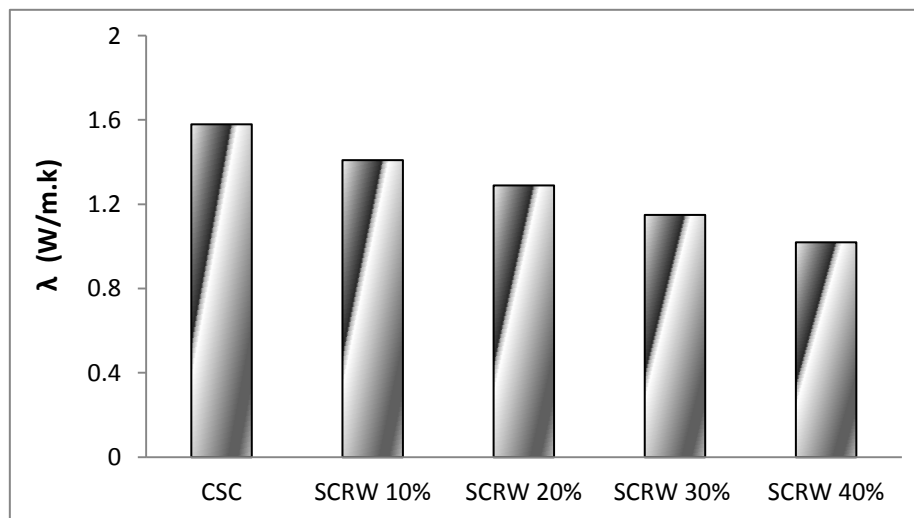


Fig.7. Thermal conductivity of sand concrete as function of rubber waste content.

#### 4. Conclusions

This paper has presented the recycling and the use of rubber wastes as aggregate in sand concrete produced either from dune sand (DS). The results which could be summarized and concluded as:

- 1-These types of rubber wastes types can be used in sand concrete.
- 2-The workability of all sand concrete increases and the density decreases with the increase of rubber waste shoes content.
- 3-The compressive and flexural strength values of all waste rubber SC mixtures tend to decrease above the values for the reference SC with increasing the waste rubber ratio. But this result was acceptable for lightweight concrete.
- 4- The addition of 40% of rubber waste in sand concrete caused a reduction (35%) in the values of thermal conductivity. This result is primarily due to lower thermal conductivity of the rubber waste, but also to the capacity of the aggregate rubber to facilitate the formation of micro voids which improves the thermal insulation performances of the sand concrete.

The use of rubber waste of shoes as aggregates in sand concrete can most of the problems associated with their disposal as well as save natural resources related to aggregates mining.

#### 5. References

- AFNOR. Concrete – Sand concrete. (1994).Projet P 18-500 [in French].
- Akçaözoğlu, S., Akçaözoğlu, K., & Atiş, C. D. (2013). Thermal conductivity, compressive strength and ultrasonic wave velocity of cementitious composite containing waste PET lightweight aggregate (WPLA). *Composites Part B: Engineering*, 45(1), 721-726.
- Ali NA., Amos AD., Roberts M.(2000). Use of ground rubber tires in Portland cement concrete. In: Proceedings of the international conference on concrete. Scotland (UK): University of Dundee.
- Eldin NN., Senouci AB.(1993). Rubber\_tyre particles as concrete aggregates. *ASCE J Mater Civil Eng.* 1993.478-96.
- Fattuhi, N. I., & Clark, L. A. (1996). Cement-based materials containing shredded scrap truck tyre rubber. *Construction and building materials*, 10(4), 229-236.
- Fedroff, D., Ahmad, S., & Savas, B. (1996). Mechanical properties of concrete with ground waste tire rubber. *Transportation Research Record: Journal of the Transportation Research Board*, (1532), 66-72.
- Guendouz, M., Debieb, F., Boukendakdji, O., Kadri, E. H., Bentchikou, M., & Soualhi, H (2016). Use of plastic waste in sand concrete.*J. Mater. Environ. Sci.* 7 (2) 382-389.
- Guendouz, M., & Debieb, F. (2015). Formulation et caractérisation d'un béton de sable à base de déchets plastiques. In 33èmes Rencontres Universitaires de Génie Civil." Bayonne, France, p 1-8.
- Goulias, D. G., & Ali, A. H. (1998). Evaluation of rubber-filled concrete and correlation between destructive and nondestructive testing results. *cement, concrete and aggregates*, 20(1), 140-144.
- Hannawi K., Kamali-Bernard S., Prince W.(2010). Physical and mechanical properties of mortars containing PET and PC waste aggregates. *Waste Management* .30.2312-20.
- Iucolano F., Liguori B., Caputo D., Colangelo F., Cioffi R.(2013). Recycled plastic aggregate in mortars composition: Effect on physical and mechanical properties. *Materials and Design*.52. 916-922.
- Khatib ZK. Bayomy FM.(1999). Rubberized portland cement concrete. *ASCE J Mater Civil Eng.*11(3) .206-13
- Lee HS., Lee H., Moon JS.(1998). Development of tire-added latex concrete. *ACI Mater J.*95(4):356-64.

- 
- Naik TR., Singh SS. Utilization of discarded tyres as construction materials for transportation facilities. Report No. (1991).CBU-02,UWM Center for By-products Utilization. Milwaukee: University of Wisconsin-Milwaukee.
- SABLOCRETE (1994). 'Béton de sable : Caractéristiques et pratique d'utilisation'. Presse de l'Ecole Nationale des Ponts et Chaussées.
- Rostami, H., Lepore, J., Silverstraim, T., & Zundi, I. (2000). Use of recycled rubber tires in concrete. In *Proceedings of the international conference on concrete* (Vol. 1993, pp. 391-399). London, United Kingdom: Thomas Telford Services Ltd.
- Siddique, R., & Naik, T. R. (2004). Properties of concrete containing scrap-tire rubber—an overview. *Waste management*, 24(6), 563-569.
- Topcu, I. B. (1995). The properties of rubberized concretes. *Cement and concrete research*, 25(2), 304-310.
-

## The effect of building materials choice on the thermal comfort in the self-produced individual housing in Biskra.

Latreche S\*, Sriti L

Department of Architecture , University of Biskra, BP 145 RP, 07000 Biskra, Algeria

\* Corresponding Author: sihem.latreche21@gmail.com

**Abstract.** The building envelope is the first barrier to protect against external climatic variations. Generally, it consists of two types of walls: opaque walls (walls and roof) and transparent walls (Windows). The design characteristics of the enclosure strongly affect the occupants' thermal comfort, as well as the building energy consumption. The constructive choices relating to structural elements, in particular, walls, roofing and openings are generally considered in the thermal exchanges between the building and its environment. In the present study, which is based on experimental analysis in the self-generated residential sector in Biskra (Algeria), where a warm and arid climate predominates, we aim to evaluate the thermal impact of certain architectural and constructive parameters that are specific to residential habitat self-produced in Biskra. This paper summarizes the main results obtained from an in situ measurement campaign that evaluated the essential parameters of thermal comfort such as ambient and surface temperature, air velocity, and humidity. These parameters were used as indicators to measure the impact of the envelope material characteristics on its climatic adaptability. This paper also presents some recommendations for optimizing the choice of building materials specific to the self-produced residential in order to improve its thermal performance while preserving the essentials of its specificities.

**Key words:** Construction materials, thermal comfort, Individual housing self-produced, hot and arid climate, Biskra.

### 1. Introduction

In Algeria, there are several reasons for the evolution of the constructive system in the individual housing, in particular the appearance of new materials and construction techniques as well as new modes of architectural design. Unfortunately, this revolution in architectural practice has ignored the specificities of the climate context, which has led to a rupture between the framework and its environment and an abusive and irrational exploitation of the resources Energy. Thus, electricity consumption in the residential sector in Algeria represents 28% of the total consumption of electricity (APRUE, 2015). This consumption is essentially, intended to cover the needs of artificial lighting, heating and air conditioning (Figure. 1); it is experiencing a growing trend in particular for the residential sector (Figure.2).

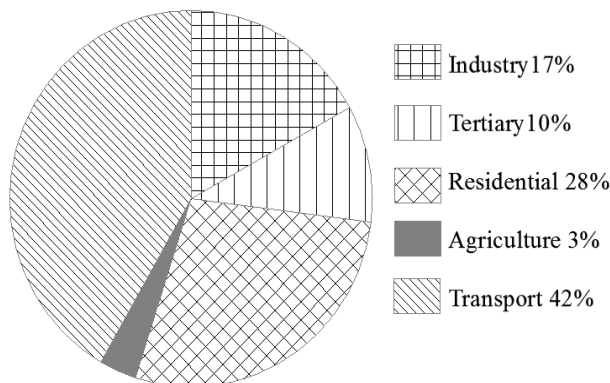


Fig. 1. Distribution of energy consumption by sector in Algeria (Source: APRUE, 2015).

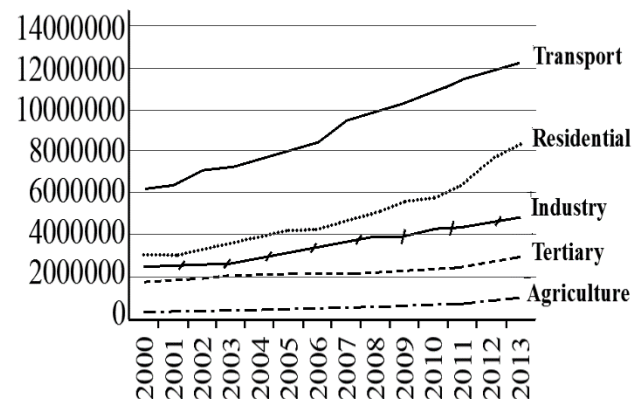


Fig. 2. Evolution of energy consumption by sector in tep (Source: APRUE, 2015).

The city of Biskra, which is characterized by a hot and arid climate, illustrates the magnitude of this phenomenon. Since a few decades, the built frame produced in this city has no relation with the climatic conditions, which drives the inhabitants to turn to the mechanical means to ensure a certain level of comfort whose cost is each year more High. In addition, it is to reduce this energy consumption and ensure optimum climatic comfort that must be taken on architectural design.

As such, the design characteristics of the envelope strongly affect the thermal comfort of the occupants, as well as the energy consumption in the building. The climate and energy performance of the envelope depends on the constructive choices relating to the structural elements, in particular the walls, the roof and the openings generally considered as determining factors in trade between the building and its environment.

The objective of this study is to evaluate the thermal impact of the structural and constructive elements of the envelope as they are used in the residential housing produced in Biskra. The ultimate goal of our research is to improve the thermal performance of the architectural envelope of this type of habitat and thus reduce energy consumption through passive solutions.

## 2. The climatic characteristics of the wilaya of BISKRA

The city of Biskra is located in the South-east of Algeria at a latitude of  $34.80^{\circ}$  North and longitude of  $5.73^{\circ}$  East (Figure. 3). Biskra belongs to a region classified arid, where a hot and dry climate with cold winters and hot summers predominates. The maximum temperature reaches  $42^{\circ}\text{C}$  during the month of July and the minimum temperature decreases to  $7^{\circ}\text{C}$  in winter during the month of January. The average annual temperature is  $21.7^{\circ}\text{C}$ , while the average annual humidity is 46%. Very low precipitation is recorded with a maximum of 20 mm/year, and an annual average of about 8.8mm/year. The directions of prevailing wind is North-west in winter, South-east in summer at a speed from 6 to 10 m/s (Figure.4).

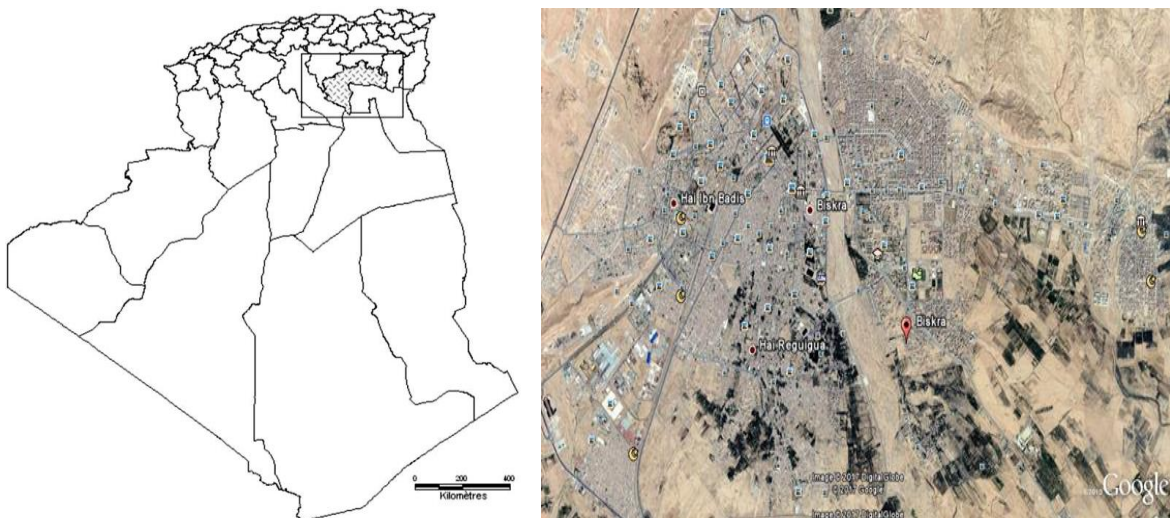


Fig 3: Situation of the Wilaya of Biskra (Source: google earth)

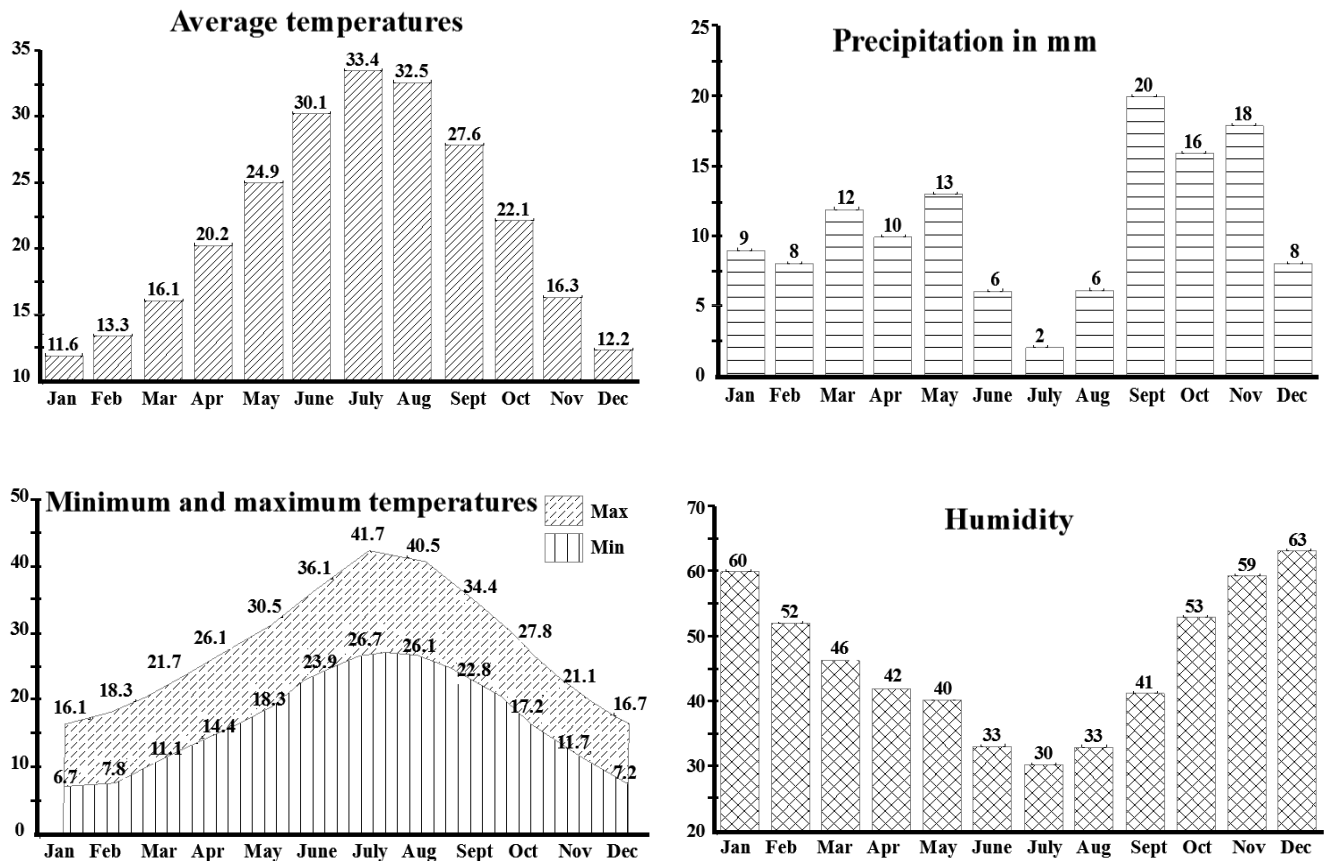


Fig 4: Climatic data of the city of Biskra (Source: Weather station data Biskra, 2000-2009)

According to Givoni (1978), to assure the hygrothermal comfort under a dry hot climate, the buildings must be adapted to the summer conditions and it assuming that a building where the comfort is assured in summer will satisfy the winter requirements. In this study, it will be limited to the presentation of the results obtained during the summer period.

### 3. The building envelope and thermal comfort

From ancient times up to the present day, the man did not stop improving his housing environment to assure a protection always more effective against weather conditions and aggressive factors of the external environment. However, thermal comfort in a building depends mainly on the thermal behaviour of its envelope (Fig. 5) More precisely are the building materials and the architectural and constructive characteristics of the structural elements (wall thickness, compositions, layout ... etc.), which determine the climatic adaptability of a construction.

The outside envelope of the building is its first barrier of protection; it consists of two types of walls: opaque walls (walls and roof) and transparent walls (Windows). The roof is responsible for 70.62% of the gains received while 27.11% of the thermal gains are transmitted by the four facades, and 2.27% by the windows (Necib, 2016). A judicious treatment of the walls of the envelope according to the warm and arid climatic conditions (choice of construction materials with high thermal inertia for walls and roofing, reduction of the dimensions of windows, solar protections ... etc.) allows to guarantee an optimal comfort inside the building, even if the outside conditions are unfavorable (Izard, 1979).

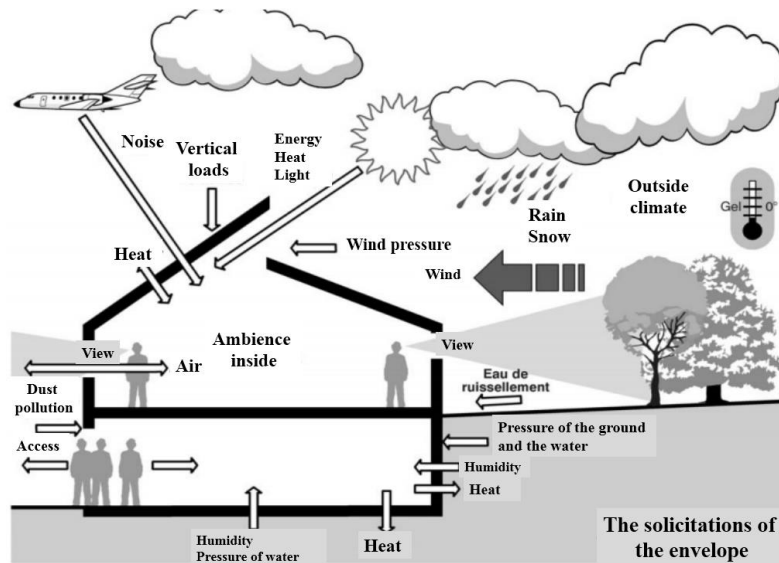


Fig. 5: The outside envelope undergoes numerous aggressions of the local climate and the environment (source: Hauglustaine, 2006)

#### 4. Experimental study

Our analytical work based on a survey in situ intended for the study of the structural and constructive parameters of the envelope influence on the thermal comfort. This one is measured from the ambient and surface temperature, the air speed, and the relative humidity. The measuring instrument TESTO was used to raise the variations of the previous three hygrothermal parameters while the surface temperature was measured with an infrared thermometer (figure. 6). The measures were made inside, outside of the room, and in various points, in particular the roof and the wall of facade (Figure.7).

To select houses to be studied, it was necessary to perform a typo-morphological analysis. An important corpus of contemporary individual self-produced in Biskra was assembled. The houses were distributed in different planned subdivisions of the city and their choice was made according to the characteristics of the most recurring envelope (orientation, building materials, ratio of openings, number of levels ... etc.). In total, 15 variants of rooms were studied.

The analysis of the climatic data of Biskra allowed us to determine the period of overheating, which is approximately one week from the end of July to the beginning of August. The recording of the measurements took place at two times of the day from 14 pm to 16 pm in the afternoon and from 9 am to 11 am in the morning.



Fig. 6 : Measuring instrument TESTO and infrared thermometer

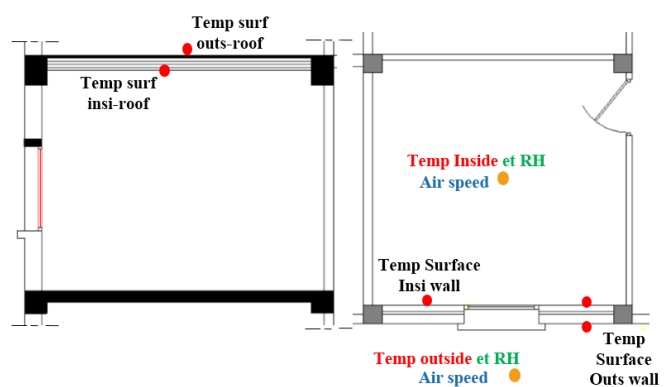
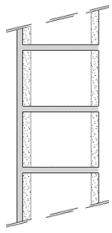

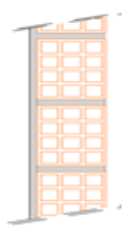
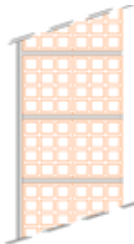
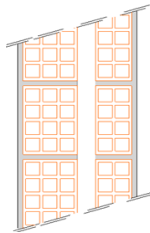


Fig. 7: Position of measurement points in the room



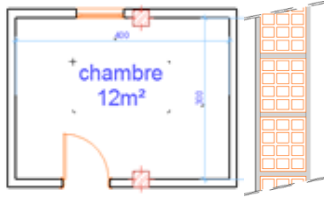

In order to study the impact of the building materials used at the envelope level, several cases have been chosen. The sample includes 15 variants that illustrate the different constructive systems of exterior walls used in the Biskra (Table 1). In addition to the walls, two other parameters have been taken into account: the orientation and position of the room in the house is in the ground floor (unexposed roof, floor), or on the upper level (exposed roof, terrace).

**Table 1: Distribution of the 15 variants of the studied pieces**

Distributions of the 15 variants of parts studied according to the construction material				
Walls in hollow perpend ( 2 variants)	Walls in full perpend ( 1 variant)	Walls simple brick-built of 15cm (4 variants in the floor)	Walls brick-built double of 15cm X2 (2var. RDC, 3var. R+1)	Walls brick with blade of air (1var double. RDC, 2var. R+1)
				

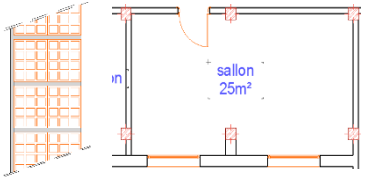
To illustrate the obtained results at the end of the campaign of measure, it was chosen to present some examples showing the parameters of thermal comfort (temperature, relative humidity, air velocity) measured in parts that differ according to Three parameters: the physical and constructive characteristics of the walls, the orientation and the type of roofing (floor or terrace) (Table 2).

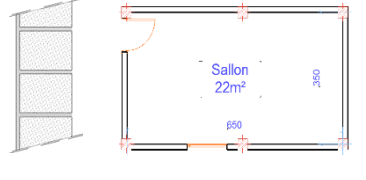
**Table 2: Examples of results of the measures made in situ in rooms using various building materials for walls;**

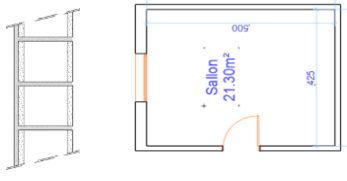
Wall in hollow brick (17cm), located on the floor, orientation South						
	Ambient temperature C °					
	Morning			Afternoon		
	Max	Min	Moy	Max	Min	Moy
Temp inside	35.2	34.6	34.8	39	36.8	38
Temp outside	39.1	33.1	37.8	44	40	41.5
Thermal gap	4	1.5	3	5	3.2	3.5
Surface temperature C °						
Temp surf insi wall	36.4	/	36.4	38.5	/	37.6
Temp surf outs wall	40.6	/	40.1	46.9	/	45.6
Thermal gap	4.2	/	3.7	8.4	/	8
Temp surf insi roof	36.8	/	36.6	37.5	/	37.5
Temp surf outs wall	42.6	/	42	41.6	/	41.2
Thermal gap	5.8	/	5.4	4.1	/	3.7
Relative Humidity %						
Humidity indoor	26.4	24.8	25.6	26.3	22.5	24.2
Humidity outside	20.3	19.7	20	14	13	13.3
Walls brick with blade of air 33cm located on the floor, orientation west						
	Ambient temperature C °					
	Morning			Afternoon		
	Max	Min	Moy	Max	Min	Moy
Temp inside	41.3	33.3	32.5	36.6	34	36.3
Temp outside	37.3	37.2	37	42.3	41	41.8
Thermal gap	4	3.9	4.5	5.7	5	5.5
Surface temperature C °						
Temp surf insi wall	37.7	/	37.6	38.5	/	38.1
Temp surf outs wall	41.6	/	41.4	49	/	48.4
Thermal gap	4	/	3.8	10.5	/	10.3
Temp surf insi roof	38.4	/	38.1	39.6	/	39.3
Temp surf outs wall	34.4	/	34.4	46.8	/	46.4
Thermal gap	4	/	3.7	7.2	/	7.1
Relative Humidity %						
Humidity indoor	25.9	24.7	25.4	20.6	20	20.3
Humidity outside	21.8	20.6	21.2	13.9	13	13.3

Air speed m / s						
Air Speed inside	0,3	0	0,1	0,3	0	0,1
Air Speed outside	1,3	0,3	0,6	1,9	0,5	1,2

Air speed m / s						
Air Speed inside	0,5	0	0,2	0,3	0	0,1
Air Speed outside	1	0,3	0,5	1,9	0,5	1,2

Wall in hollow brick 15+15 (32 cm), located on the floor, orientation North-west						
	Ambient temperature C °					
	Morning			Afternoon		
	Max	Min	Moy	Max	Min	Moy
Temp inside	35,3	35,3	35,3	38	37,6	37,8
Temp outside	39,6	38	39,2	42,8	34,3	42,6
Thermal gap	4,3	2,7	4	4,8	3,3	4,8
Surface temperature C °						
Temp surf insi wall	35	/	34,1	38,5	/	38
Temp surf outs wall	38,3	/	36,5	45,5	/	44,7
Thermal gap	3,3	/	2,4	7	/	6,7
Temp surf insi roof	38,4	/	38,4	38,8	/	38,7
Temp surf outs wall	35,8	/	34,7	47,5	/	47,1
Thermal gap	2,6	/	3,7	8,7	/	8,4
Relative Humidity %						
Humidity indoor	30,7	26,7	29	26,7	20	21,8
Humidity outside	23,2	20,4	21,6	15,4	14,8	15,5
Air speed m / s						
Air Speed inside	0,3	0	0,1	0,3	0	0
Air Speed outside	1,9	0,3	0,7	0,5		0,3

Walls in full perpend (20cm) located on the ground floor, orientation west						
	Ambient temperature C °					
	Morning			Afternoon		
	Max	Min	Moy	Max	Min	Moy
Temp inside	37,4	37	37,1	40,3	40,1	40,2
Temp outside	40	39	39,7	41,5	40,8	41
Thermal gap	2,6	2	2,6	1,2	0,7	0,8
Surface temperature C °						
Temp surf insi wall	36,4	/	37,1	42,1	/	41,7
Temp surf outs wall	41,2	/	41	45,4	/	45
Thermal gap	4,8	/	3,9	3,3	/	3,3
Temp surf insi roof	37,1	/	37	44,7	/	44,3
Temp surf outs wall	39,2	/	38,6	50,6	/	49
Thermal gap	2,1	/	1,6	5,9	/	4,7
Relative Humidity %						
Humidity indoor	31,1	24,2	26,1	21,4	19	19,6
Humidity outside	21,8	21,6	21,7	19,4	17,5	18,2
Air speed m / s						
Air Speed inside	0	0	0	0	0	0
Air Speed outside	1,4	0,4	0,8	0,5	0	0,3

Walls in hollow perpend (22cm) located on the ground floor south-west orientation						
	Ambient temperature C °					
	Morning			Afternoon		
	Max	Min	Moy	Max	Min	Moy
Temp inside	32,2	32	32,1	37,7	34,7	36,5
Temp outside	34,8	34	34,3	41,1	38,4	37,5
Thermal gap	2,6	2	2,2	3,4	0,5	1
Surface temperature C °						
Temp surf insi wall	31,5	/	31,2	37,2	/	36,9
Temp surf outs wall	35,8	/	35,4	45,7	/	45
Thermal gap	4,3	/	4,2	8,5	/	8,1
Relative Humidity %						
Humidity indoor	39,4	34,8	35,6	32,1	26,2	29,4
Humidity outside	32,8	31,3	31,8	21,5	17,9	20
Air speed m / s						
Air Speed inside	0,5	0	0,1	0,6	0,0	0,1
Air Speed outside	2,1	0,3	1	2,6	0,3	1

## **5. Interpretation of the results**

### ***5.1 Air temperature***

According to Bennadji (1999), the subtraction of the external average temperatures from those of the interior of the room allows to appreciate the temperature difference between the inside and the outside. In table 2, it is noted that there is a difference of 0.5 C ° to 2 C ° between these two temperatures in a house built in single wall (single partition). The maximum value of ambient temperature is recorded in houses built in hollow and full block; for these cases, the indoor temperature is in the order of 32 ° to 38 ° at the time when the outside temperature reaches the 40 °. This constructive choice is visibly inadequate for the warm and arid climate. For the rooms built on the floor the situation of discomfort is at its extreme, for example for a piece built in single 15 cm brick wall, the average temperature difference is in the order of 3 C ° to 3.5 C °.

On the other hand, in the houses built in double partition, the temperature difference is more appreciable. As an example, for double brick walls of 15 cm, it is between 4 C ° to 4.5 C ° (the internal temperature reaches 23.5 C °, outside it is 26.5 C °). In the case of double walled walls with a blade of air, the thermal gap between the inside and outside is optimal in the order of 5 C to 5.5 C °.

In conclusion, it appears that the highest indoor temperatures are recorded in simple walled rooms with low thermal resistance materials such as hollow and full block. On the other hand, the walls in double walls give more interesting results from the point of view of thermal comfort in the summer period. Note that the ambient temperatures measured are also dependent on other factors such as orientation and external climatic fluctuations.

### ***5.2. The relative humidity and the air speed***

When reading the results of the measurements, we can be said that the external relative humidity is low compared to the internal humidity, on the outside it usually varies between 15% and 19% and inside it is between 22% and 31%. These results can be explained by human metabolism vapor and domestic activities and also the lack of aeration in the house.

According to Liebard (2005), the air velocity that does not exceed 0.2 m/s in the habitat has an influence on convective heat exchanges. However, with respect to the parts tested, the air velocity was very low not exceeding 0.1 m/s due to the lack of transverse ventilation.

### ***5.3. The values of the surface temperature***

According to Szokolay (2004), the temperature of the external surface has great effects on the internal thermal conditions; moreover, it varies with the clarity of the color and the velocity of the air in contact with the surface. Based on the results obtained, it appears that the temperatures of the internal surfaces are higher than the ambient temperature when the walls are exposed to solar radiation. Thus, the higher the external surface temperature increases due to the lack of shading and the lack of solar protections at the level of openings, the higher the ambient temperature rises in proportion to the external surface temperature. The temperature of the air and the surface temperature are therefore linked both by the amount of the incident solar radiation and also by the thermo-physical properties of the building materials, which retard the transfer of the heat inside.

---

---

## 6. Conclusions

Through an experimental in situ study of a single-detached houses corpus in Biskra, the influence of the structural and constructive choices of the architectural envelope on the inner thermal comfort was examined. This experiment has shown that a judicious choice of materials can positively influence the inner thermal comfort, especially thanks to the thermo-physical properties of the materials that allow regulating heat exchanges between the building and its environment. The double-walled walls offer some advantages from the point of view of thermal comfort during the summer period. Moreover, the thermal operation of the enclosure can be optimized thanks to the integration of the solar protections according to the orientation of the façade.

## 7. References

- APRUE, (2015). Final energy consumption of Algeria, key figure-year 2015; Ministry of Energy and Mines.
- Bennadji, A. (1999). Climatic or cultural Adaptation in arid zones: case of the Algerian South-East. PhD thesis. Université d'Aix-Marseille1-Université de Provence.
- Hauglustaine J.-M. (2006). The Global Conception of the envelope and the energy, a practical Guide for architects; Ministry of the Walloon Region; February 2006.
- Givoni, B. (1978). Man architecture and climate. Editions Le Moniteur, Paris, France, 460 p.
- Izard, J. L. (1979). Archi Bio; Editions parentheses; Roquevaire, 1979.
- Liebard, A. (2005). Treatise on Bioclimatic Architecture and urbanism: design, build and develop with sustainable development. Editions Le Moniteur, Paris, France, 2005.
- Necib, H (2016). Improved thermal insulation of habitats in warm and arid regions. Third International Conference on Energy, materials, Applied Energetic And Pollution. ICEMAEP 2016; Constantine, Algeria
- Szokolay, V. (2004). Introduction to architectural science, the basis of sustainable design. Architectural Press Edition, edition An imprint of Elsevier Science, 348p.
-

## Development of materials based on PET-siliceous sand composite aggregates

Gouasmi M.T.<sup>1,\*</sup>, Benosman A.S.<sup>1,2,3</sup>, Taïbi H.<sup>1</sup>

1 Faculty of Exact and Applied Sciences, Laboratory of Polymer Chemistry LCP, University of Oran 1, Ahmed Benbella, BP 1524, El Mnaouer, Oran 31000, Algeria.

2 Higher School of Applied Sciences, ESSA-Tlemcen, Bel Horizon, 13000 Tlemcen, Algeria.

3 Department of Civil Engineering, Laboratory of LABMAT, ENPO Maurice Audin, Oran, Algeria.

\* Corresponding Author: [m.t.gouasmi@hotmail.fr](mailto:m.t.gouasmi@hotmail.fr)

---

**Abstract.** Plastic waste recycling for the development of new building materials, such as cementitious composites, appears to be one of the best solutions to get rid of this type of waste. This operation has many economic and ecological advantages. The present study proposes some solutions for the recovery of plastic waste from PET (polyethylene terephthalate) bottles in order to obtain, after heat treatment at 290 °C followed by step cooling, a light composite material (PET-siliceous sand) with a hardness close to that of natural rock. The structure of the material obtained is characterized first; then the effect of this composite, with different substitution rates of natural aggregate, on the behavior of an industrial screed is studied. Afterwards, some specific recommendations for the uses of this screed, and possibly of the composite itself, are given. Although the main effects of certain polymeric additives on the mechanical properties of mortars are known, the mechanisms that are responsible for these effects are not yet well understood. Techniques such FTIR, XRD, SEM and differential scanning calorimetry (DSC) are analytical tools that can be used for the characterization and expertise of this type of composites, particularly the industrial composite screeds. Results from the present article enabled us to state that the composition of the materials obtained remains qualitatively unchanged and that no chemical interaction was observed between the mineral species and the waste PET lightweight aggregate (WPLA) or the composite itself; in fact, no new compounds were formed. In addition, the differential scanning calorimetry (DSC) technique allowed us to conclude that the addition of WPLA has an influence on cement hydration. The thermo-mechanical characterization of WPLA made it possible to observe an excellent arrangement between the PET and siliceous sand. Therefore, the development of WPLA may be another solution for a number of applications in the field of eco-materials for construction and building.

---

**Key words:** Green/eco composite; Recycled materials; PET polymer; WPLA (Waste PET Lightweight Aggregate); Microstructural analyses.

### 1. Introduction

In the field of construction, a screed is a mortar layer made of cement, resin or lime, applied on the ground and intended to flatten, level, come on a support and / or coat elements, such as a heating floor, and then to receive the upper layers, like tiles, a flexible floor, a floating or glued floor (Fiches Techniques G11, 2013). Depending on the design and method of execution, two different types of screeds may be mentioned, namely the adhering screeds, which are incorporated or attached, and the floating screeds. The use of polymer waste in building materials has been evolving for decades. Various kinds of screeds, composite mortars and concretes, plastic aggregates (Alfahdawi et al. 2016; Gu and Ozbakkaloglu, 2016) and composite aggregates WPLA (Akçaözoglu et al. 2013; Choi et al. 2009; Zuccheratte et al. 2017) have been formulated so far. These new applications came to respond to specific demands expressed by building and civil engineering professionals, in particular for the acoustic and thermal comfort and durability.

The aim of the present work is to present the results of a first experimental study on the characterization of the structure obtained using IRTF, XRD, SEM techniques as well as thermal analysis techniques, such as DSC, for building elements, like screeds made of composite aggregates (PET- siliceous sand), which contain crushed PET waste. These composite aggregates are used as substitutes for natural aggregates in order to make an industrial composite screed. This represents an important contribution to sustainable development. Some optimal substitution proportions have been studied as well in order to determine the feasibility limits, unlike what has been undertaken in previous works (Alqahtani et al. 2014, 2017; Choi et al. 2005, 2009; Zuccheratte et al. 2017). In general, the WPLA aggregate composites obtained seem to be inexpensive materials that could help solve some solid waste disposal problems, in addition to the energy gain they can generate.

## 2. Experimental program

### 2.1 Cement

The type of cement used is Matine 42.5 CPJ CEM II/A, from Lafarge Cement Plant, based in Oggaz (North-West of Algeria). This cement has a fineness of 4500 cm<sup>2</sup>/g, absolute density of 3.09 g/cm<sup>3</sup> and average compressive strengths of 22 MPa at 2 days, and 48 MPa at 28 days. The chemical composition of cement, siliceous sand (S<sub>s</sub>) and calcareous sand (C<sub>s</sub>) as well as the mineralogical composition of clinker are given in Tables 1 and 2, respectively.

Table 1. Elementary chemical composition of CPJ 42.5 cement, siliceous (S<sub>s</sub>) and calcareous (C<sub>s</sub>) sands, wt. %

Oxides	Cement	S <sub>s</sub>	C <sub>s</sub>
SiO <sub>2</sub>	17.40	83.29	11.76
Al <sub>2</sub> O <sub>3</sub>	4.12	0.21	–
Fe <sub>2</sub> O <sub>3</sub>	2.97	0.45	0.91
CaO	61.15	7.03	44.35
MgO	1.16	4.2	–
K <sub>2</sub> O	0.66	–	–
SO <sub>3</sub>	2.46	–	–
Na <sub>2</sub> O	0.13	–	–
LOI	8.85	–	–
Cl <sup>-</sup>	0.017	–	–
CaCO <sub>3</sub>	–	2.27	59.09
CO <sub>2</sub>	–	1.00	26

LOI: loss on ignition.

Table 2. Mineralogical composition of clinker (%w)

C <sub>3</sub> S	C <sub>2</sub> S	C <sub>3</sub> A	C <sub>4</sub> AF
64	15	8	12.16

### 2.2 Thermomechanical protocol for the preparation of the composite aggregate WPLA (Waste PET Lightweight Aggregate)

It is a combination of a natural element, i.e. silica sand, and upgraded waste PET bottles. Heat treatment followed by a stepwise cooling is required in order to have slices with hardness close to that of natural rock (Figure 1a). These fragments undergo an industrial grinding, giving different granular fractions; the one used in this study is 0/0.3 (Figure 1b). The chemical composition of silica sand used and the XRD analysis, MOP picture of WPLA microstructure are shown in Table 1 and Figures 1c,d, respectively.

### 2.3 Calcareous sand

The calcareous sand (CS), which will be substituted by the composite aggregate WPLA throughout this study, is a calcium-silicate sand from SECH quarries of HASNAOUI Group, based at Sidi Ali Benyoub (Wilaya of Sidi Bel Abbes, Algeria). The chemical composition of the sand used, is shown in Table 1.

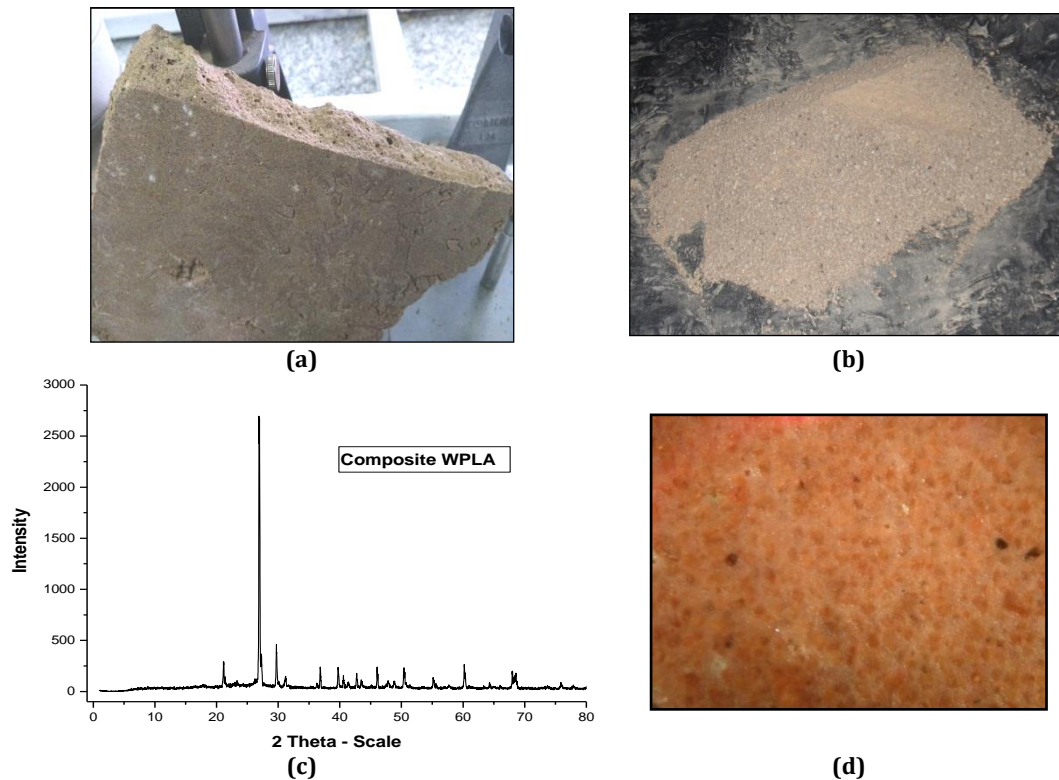


Fig 1. (a) Slices, (b) Granular fractions, (c) XRD spectrum and (d) Optical Microscope picture (4.8x) of the WPLA composite aggregate

### 2.4 Test Methods

It was Granular mixtures for the preparation of composite screed mortars were prepared from Matine cement, and four combinations were obtained by partial and total replacement of the starting silico-calcareous sand by 25%, 50%, 75% and 100% by weight of the WPLA composite aggregate previously prepared. For each formulation, the mixtures were prepared based on Standard ASTM C109-11 (2011), in order to fabricate specimens with dimensions  $5 \times 5 \times 5 \text{ cm}^3$ . These mixtures were composed of one third of binder (cement) and two thirds of aggregates with respect to the overall weight. These aggregates are calcareous sand and WPLA. The water to cement (W/C) ratios used allowed for workability values between 85 and 105. The maneuverability of each type of the formulated mortars was measured according to Standard ASTM C 1437 (2001), using the spreading table test. The molds containing the samples were covered with a plastic film and stored in the maturation cabinet of the laboratory. After 24 hours, the samples were unmolded and immersed in lime-saturated water (ASTM C511, 2006), for 28 days, at the temperature of  $20 \pm 2^\circ\text{C}$ . The compression and flexural strengths of the samples were measured using a hydraulic press after 28 days (NFEN 196-1, 2005).

The characterization of the previous materials, conserved in water, was carried out using various analytical techniques, such as the Differential Scanning Calorimetry (DSC) Thermal Analysis which was carried out in the laboratory of CHIALI Group, located in the industrial zone of the town of Sidi Bel Abbes. The apparatus used is a differential scanning calorimetric analyzer (DSC, NETZSCH DSC 200PC, with temperature rise ramps equal to  $10 \text{ K / min}$ , up to  $600^\circ\text{C}$ ,

under nitrogen flux). Test samples of mortar, composite, siliceous sand and PET were analyzed according to linear heating, starting from ambient temperature up to 600 °C, with a heating rate of 10 K/min. The analysis of the samples was carried out on an attenuated total reflection (ATR) patch, using a Spectrum One PerkinElmer FT-IR spectrometer. The FT-IR spectra were obtained by applying the FTIR-ATR infrared spectrometry technique to the samples for a few minutes. The SEM and XRD analyses were performed using a HITACHI TM-1000 apparatus and a Bruker D8 ADVANCE diffractometer (Cu-K $\alpha$ ), respectively.

### 3. Results and discussion

#### 3.1 Interpretation of FTIR spectra of the composite aggregate and composite screed mortars

The polymer PET is characterized by the presence of the following remarkable absorption bands (Figure 2a):

- around 867.3 cm<sup>-1</sup> (out-of-plane or para-disubstituted alternating cycle deformations),
- near 1095.8 cm<sup>-1</sup>, due to the vibrations of the -CO- bond,
- at 1577.9 cm<sup>-1</sup> and 1616.1 cm<sup>-1</sup>, due to the vibration modes of the benzene ring,
- around 1715.8 cm<sup>-1</sup>, due to the grouping -COO-,
- at 2858.0 cm<sup>-1</sup> and 2924.0 cm<sup>-1</sup>, characteristic of the bonds -CH<sub>2</sub>-,
- Around 3002.2 cm<sup>-1</sup>, due to the valence vibrations  $\nu$ CH of the benzene ring (Figure 2a).

It is important to mention that the amount of the valorized polymer (PET) is much less than that of silica sand in the WPLA composite aggregate. This component (PET) is completely masked by the vibrations of the siliceous sand bonds. These vibrations are present in the spectrum of the WPLA composite (in Figure 2, presence of broad and intense absorption bands around 1200 cm<sup>-1</sup> 1600 cm<sup>-1</sup>, and especially around 910 cm<sup>-1</sup>, which is characteristic of the Si-O bond of silica, Figure 2b).

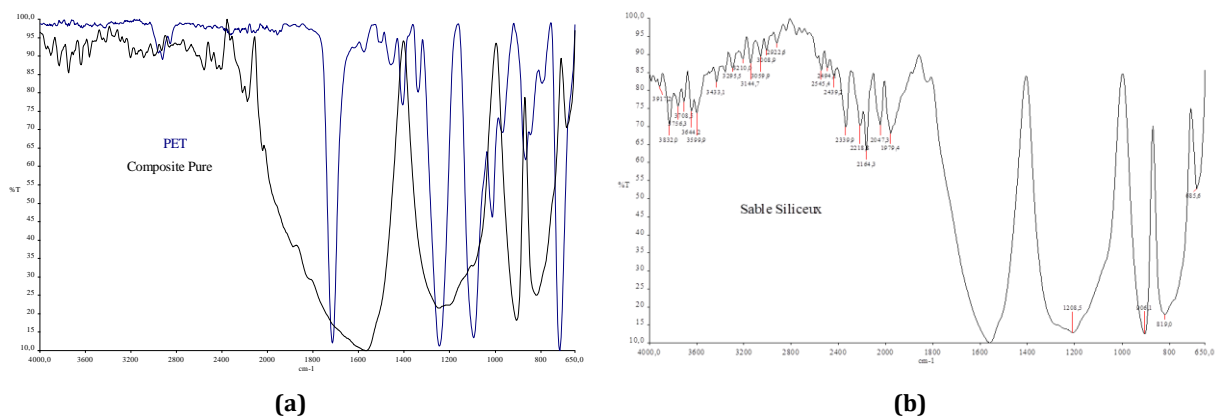


Fig 2. (a) Superposition of FTIR spectra of PET and composite aggregate, (b) FTIR spectra of siliceous sand.

Figures 3 and 4 display the superposition of FTIR spectra of samples of PET, composite aggregate, WPLA0 and WPLA100. The spectra are distinguished by the presence of specific lines for PET, composite aggregate and WPLA100. It is found that the characteristic lines of the Waste PET Lightweight Aggregate (WPLA) correspond exactly to those observed on the WPLA100. The lines characterizing the PET are masked by those of the WPLA composite, as shown in Figure 4.



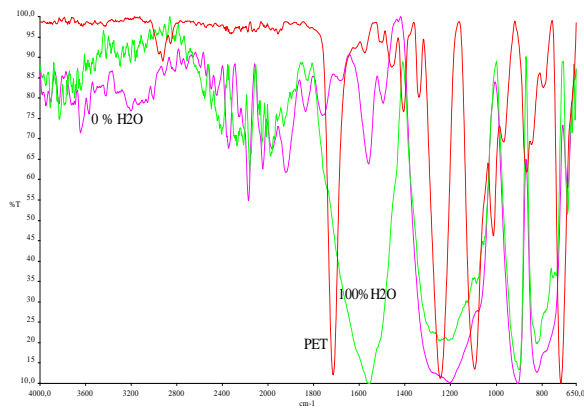


Fig 3. Superposition of the FTIR spectra of the samples WPLA0, WPLA100 and PET (Gouasmi et al. 2017).

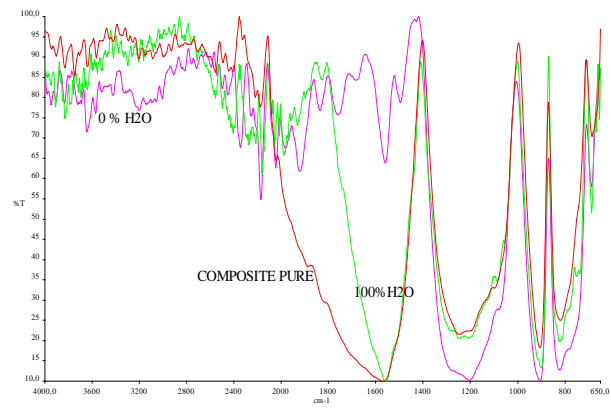


Fig 4. Superposition of the FTIR Spectra of the samples WPLA0, WPLA100 and composite aggregate.

All the spectra obtained for the composites showed the same lines, more or less intense, depending on the WPLA composite aggregate content, as shown in Figure 5. In view of the high number of results, it was necessary to reduce the number of spectra relating to samples WPLA50 and WPLA75. Moreover, it was found that there is no chemical interaction between the inorganic compounds and the organic molecules, and therefore no new compounds were formed. This corroborates the results previously reported by Benosman et al. (2012) and Zuccheratte et al. (2017).

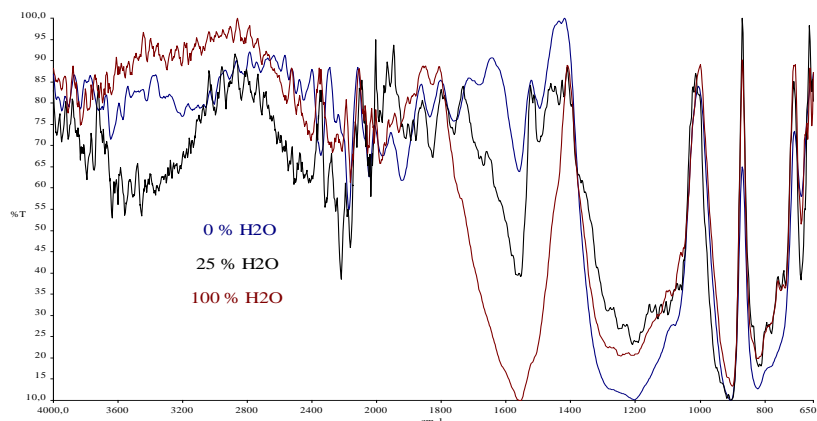


Fig 5. Superposition of the FTIR spectra of samples WPLA0, WPLA25 and WPLA100.

### 3.2. Scanning Electron Microscopy (SEM) microstructural analysis

The visualization of the microstructure of the PET-siliceous sand interface is illustrated in Figure 6 (SEM photo). The thermomechanical preparation of the WPLA composite aggregates allowed having a good adhesion and an excellent arrangement between the plastic PET waste and siliceous sand, as shown in Figure 6.

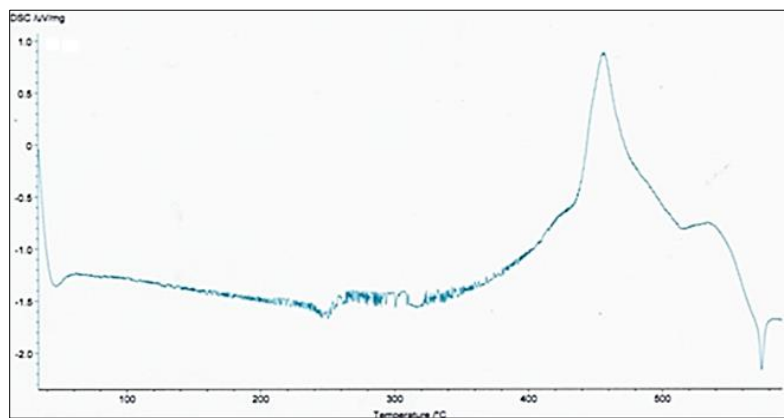


Fig 6. Microstructure of the PET- siliceous sand interface in the samples of the WPLA composite using SEM.

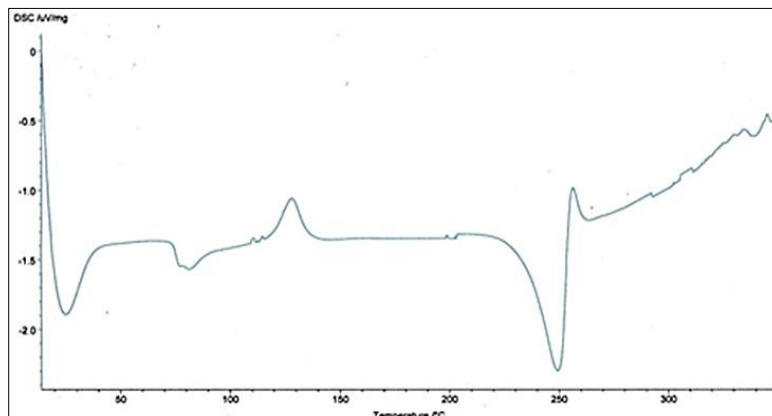
### 3.3. Differential scanning calorimetry (DSC)

Some research (Kameche et al. 2009; NFT01-021, 1974; Platret and Deloye, 1994) has reported the identification, by thermal analysis techniques, such as DSC, ATD and ATG, of cement hydration products such as C-S-H gel, portlandite, ettringite, gypsum and calcite. Therefore, Silva et al. (2002) used the ATD analysis and showed the different changes resulting from the incorporation of Ethylene Vinyl Acetate (EVA) copolymer in composite materials. Similarly, Benosman et al. (2012) applied the ATD technique and reported the different alterations resulting from the addition of polyethylene terephthalate (PET).

The DSC curve (Figure 7 a) relative to siliceous sand presents two peaks; one is endothermic, around 570 °C, and is due to the  $\alpha$ - $\beta$  phase transformation of quartz; the other one is exothermic and is found between 450 °C and 460 °C. Polyethylene terephthalate (PET) is characterized by the three: vitreous, crystalline and melting phases corresponding to the three temperatures of 80 °C, 130 °C and 250 °C, respectively (Figure 7 b).



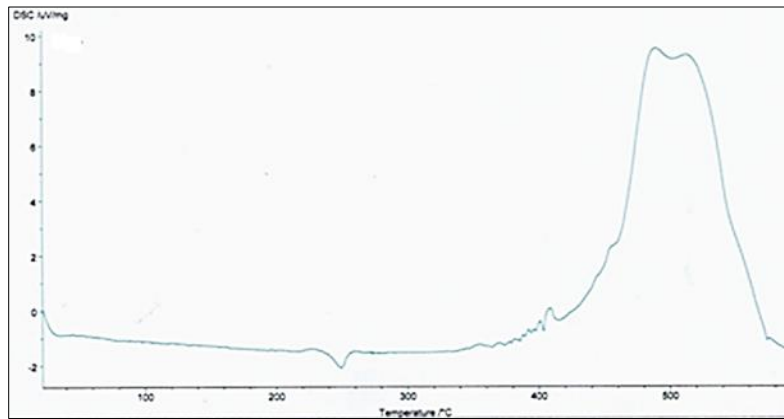
(a)



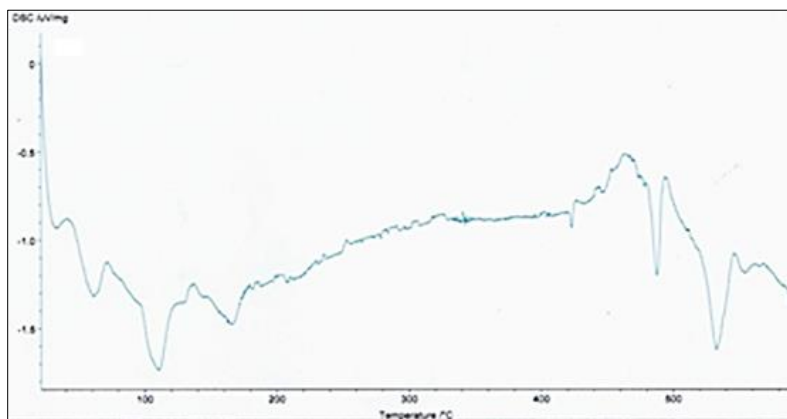
(b)

Fig 7. DSC curves, with a heating rate of 10K/min, of: (a) siliceous sand, and (b) PET.

The characterization of the WPLA composite by the DSC technique (Figure 8a) indicates the presence of PET, which is confirmed by the presence of an endothermic peak corresponding to the melting temperature around 250 °C and an intense exothermic peak between 460 °C and 520 °C (this peak is also observed in the case of siliceous sand).



(a)

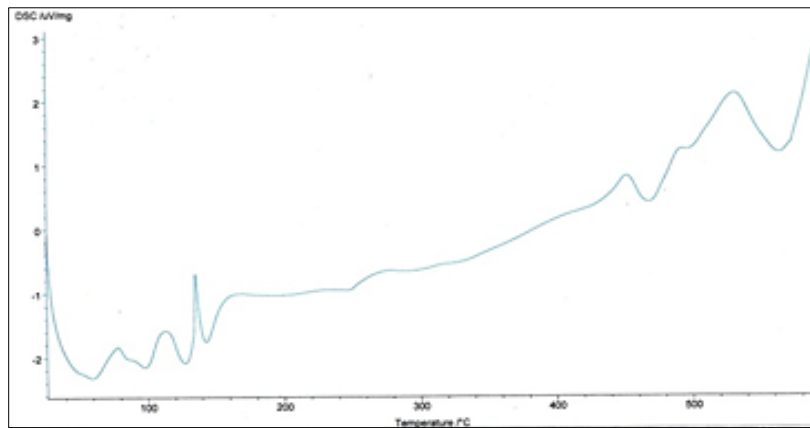


(b)

**Fig 8.** DSC curves, with a heating rate of 10K/min, of: (a) WPLA composite aggregate, and (b) WPLA0 stored in fresh water.

The DSC curves, obtained for all tests, are typical for hydrated cement pastes (Figures 8b and 9). Five major endothermic reactions occurred, during the sample heating, as follows:

- Between 30 and 105 °C: free water and some of the adsorbed water escaped from mortar. It was completely removed at 105 °C,
- Between 100 and 200 °C: various dehydration stages of C-S-H and ettringite were observed,
- At 140 °C: decomposition of gypsum  $\text{CaSO}_4 \cdot 2\text{H}_2\text{O}$ ,
- Between 175 and 190 °C: hydration of calcium monocarboaluminate,
- Between 470 and 500 °C: dehydration of portlandite  $\text{Ca}(\text{OH})_2$ .



**Fig 9. Differential Scanning Calorimetry (DSC) Thermal Analysis of WPLA50 immersed in water.**

The incorporation of the WPLA (PET-siliceous sand) composite into polyphase materials affects the DSC curve, as this can be seen in Figure 9. Peaks are observed:

- Between 30 and 105 °C: free water and some of the adsorbed water escaped from mortar. It was completely removed at 105 °C,
- Between 100 and 200 °C: various dehydration stages of C-S-H and ettringite were observed,
- An exothermic peak was found at 130 °C; it characterizes the crystallization temperature  $T_c^\circ$  of PET,
- Around 140 °C: decomposition of gypsum  $\text{CaSO}_4 \cdot 2\text{H}_2\text{O}$ , probably concealed by the peak of crystallization temperature  $T_c^\circ$  of PET,
- Decrease in the intensity of the endothermic peak for the dehydration of calcium hydroxide ( $\sim 455$  °C),
- The melting temperature of PET was observed at 255 °C,
- Significant changes were noted on the DSC curve, for temperatures above 500 °C (an exothermic shoulder was detected between 510 and 520 °C). This is certainly due to the presence of the WPLA composite,
- An endothermic peak was found around 565 °C, surely resulting from the transformation of the structure from quartz  $\alpha$  into quartz  $\beta$ , indicating the presence of siliceous sand.

These results confirm those previously reported by Benosman et al. (2016).

#### 4. Conclusions

On the basis of the above, the following conclusions can be drawn:

- Analytical methods, such as FTIR, XRD, SEM and DSC, revealed that the composition of the materials studied remained qualitatively unchanged and that the chemical interactions between the mineral species and the WPLA aggregate or the composite itself did not lead to the formation of new compounds. As part of a first attempt to evaluate an unknown material, the FTIR spectrometry could provide a wealth of interesting information which was later confirmed by analytical means, better suited to the cases to be treated.
- From the thermogravimetric studies previously carried out, the results of which are illustrated by the DSC curves, it can be concluded that the addition of the PET-based WPLA composite aggregate has an impact on the hydration of cement.

- The thermomechanical development of the WPLA composite aggregates enabled us to obtain a good adhesion and an excellent arrangement between the PET plastic waste and siliceous sand. A rough surface of the composite aggregate was obtained; it exhibited better adhesion and a larger contact area between the WPLA and the cementitious matrix (Gouasmi et al. 2015a). Thus, it can be said that the incorporation of PET lead to a densification of the cementitious matrix, and consequently a significant improvement in the durability of the material.

The use of composite aggregates containing PET waste and siliceous sand in building materials seems to be feasible given the interesting results obtained during the analysis of their properties. Positive results have been obtained by the author (Gouasmi et al. 2015a,b, 2016) concerning the use of this composite aggregate in building materials. This study is certainly a valuable contribution to the PET waste recycling program and the reduction of pollution in order to preserve the environment.

## Acknowledgments

We would like to acknowledge the financial contribution within the framework of the Algerian project CNEPRU B00L01UN310120130068. The authors would also like to thank the HASNAOUI Group of Companies, TEKNACHEM Algeria and the late Ahmed TALEB. Furthermore, the authors would like to warmly thank Mr. M. Benabadji for the Proofreading and Linguistic Review of this paper.

## 5. References

- Akçaözöğlü, S., Akçaözöğlü, K., & Atiş, C.D. (2013). Thermal conductivity, compressive strength and ultrasonic wave velocity of cementitious composite containing waste PET lightweight aggregate (WPLA). *Composites: Part B*, 45, 721–726.
- Alfahdawi, I.H., Osman, S.A., Hamid, R., & Al-Hadithi, A.I., (2016). Utilizing waste plastic polypropylene and polyethylene terephthalate as alternative aggregates to produce lightweight concrete: a review. *Journal of Engineering Science and Technology*, 11(8) 1165-1173.
- Alqahtani, F.K., Ghataora, G., Khan, M.I., & Dirar, S. (2017). Novel lightweight concrete containing manufactured plastic aggregate, *Construction and Building Materials*, 148, 386–397.
- Alqahtani, F.K., Khan, M.I., & Ghataora G. (2014). King Saud University, Synthetic aggregate for use in concrete. U.S. Patent 8, 921, 463. <https://www.google.com/patents/US8921463>
- ASTM C109/C109M. (2011). Standard Test Method for Compressive Strength of Hydraulic Cement Mortars (Using 2-in. or [50-mm] Cube Specimens), ASTM, Philadelphia, United States.
- ASTM C1437-01. (2001). Standard Test Method for Flow of Hydraulic Cement Mortar, ASTM, Philadelphia, United States.
- ASTM C511-06. (2006). Standard Specification for Mixing Rooms, Moist Cabinets, Moist Rooms, and Water Storage Tanks Used in the Testing of Hydraulic Cements and Concretes, ASTM, Philadelphia, United States.
- Benosman, A.S, Mouli, M., Taïbi, H., Belbachir, M., Senhadji, Y., Behloui, I., & Houivet, D. (2012). Mineralogical study of Polymer-Mortar Composites with PET polymer by means of spectroscopic analyses. *Materials Sciences and Applications*, 3(3), 139-150.
- Benosman, A.S., Taïbi, H., & Mouli, M. (2016). Performances Mécaniques et Durabilité des Composites Mortier-PET, Recherche et Développement dans la Revalorisation et l'Application des Déchets du PET en Génie Civil. Maison d'édition : Editions universitaires européennes EUE.
- Choi, YW., Moon, DJ., Chung, JS., & Cho, SK. (2005). Effects of waste PET bottles aggregate on the properties of concrete. *Cement and Concrete Research*, 35, 776-781.

- 
- Choi, YW., Moon, DJ., Kim, YJ., & Lachemi, M. (2009). Characteristics of mortar and concrete containing fine aggregate manufactured from recycled waste polyethylene terephthalate bottles. *Construction and Building Materials*, 23, 2829-2835.
- Fiches Techniques, G11. (2013). Les bétons : formulation, fabrication et mise en œuvre, ed, Collection technique CIMbéton, T.2, Chap.1. pp. 22-25.
- Gouasmi, M.T., Benosman, A.S., Taïbi, H., & Belbachir, M., & Senhadji Y. (2015b). Effect of a Composite Aggregate on the Durability of Mortars. *Journal of Chemistry and Materials Research*, 3, 26–31.
- Gouasmi, M.T., Benosman, A.S., Taïbi, H., Belbachir, M., & Senhadji Y. (2016). The physico-thermal properties of mortars made of composite aggregates "PET- siliceous sand". *Journal of Materials and Environmental Science*, 7(2), 409-415.
- Gouasmi, M.T., Benosman, A.S., Taïbi, H., Belbachir, M., Senhadji, Y., & Mouli, M. (2015a). Application des Agrégats Composites Légers dans les Mortiers : Cas d'une Chape Industrielle. In *Proceedings of 2nd International Symposium CIMDD'2015*, University M'hamed Bougara Boumerdes, Algeria (9-10 Nov.), (ISBN: 978-9931-9090-6-2).
- Gouasmi, M.T., Benosman, A.S., Taïbi, H., Kazi Tani, N., & Belbachir, M. (2017). Destructive and Non-destructive testing of an industrial screed mortar made with lightweight composite aggregates WPLA. *International Journal of Engineering Research in Africa*, 33, 140-158.
- Gu, L., Ozbakkaloglu, T. (2016). Use of recycled plastics in concrete: A critical review. *Waste Management*, 51, 19-42.
- Kameche, Z.A., Kazi Aoual, F., Semcha, A., & Belhadji M. (2009). Effets des hautes températures sur le comportement du béton: application au revêtement des tunnels. In the *Proceedings of the 1st International Conference SBEIDCO*, 1, 199, ENPO Oran, Algeria, (12-14 Oct.). (ISSN 2170-0095).
- NF EN 196-1. (2005). Methods of testing cement - Part 1: determination of strength, CEN.
- Norme NF T01-021. (1974). Analyse thermique: Vocabulaire - Présentation des résultats, décembre.
- Platret, G., & Deloye, F.X. (1994). Thermogravimétrie et carbonatation des ciments et des bétons, *Acte des Journées des Sciences de l'Ingénieur*. 1, 273, Giens, France (4-7 Octobre).
- Silva, D.A., Roman, H.R., & Gleize, P.J.P. (2002). Evidences of chemical interaction between EVA and hydrating Portland cement. *Cement and Concrete Research*, 32, 9, 1383-1390.
- Zuccheratte, A.C.V., Freire, C.B., & Lameiras, F.S. (2017). Synthetic gravel for concrete obtained from sandy iron ore tailing and recycled polyethylthephtalate. *Construction and Building Materials*, 151, 859-865.
-

## Behaviour of reinforced columns with E\_Glass fiber and carbon fiber

Bouchelaghem H<sup>1,2,\*</sup>, Bezazi A<sup>2</sup>, Boumaaza M<sup>3</sup>, Benzanache N<sup>3</sup>, Scarpa F<sup>4</sup>

- 1 Department of Mechanical Engineering, Faculty of Science of Technology, Mentouri Brothers University, Constantine 25000, Algeria.
  - 2 Laboratory of Applied Mechanics of New Materials (LMANM), University 8 May 1945, BP 401 Guelma 24000, Algeria.
  - 3 Laboratory of Civil and Hydraulic Engineering (LGCH), University 8 May 1945, BP 401 Guelma 24000, Algeria.
  - 4 Department of Aerospace Engineering, University of Bristol, BS8 1TR Bristol, UK.
- \* Corresponding Author: [bouchelaghem\\_h@yahoo.fr](mailto:bouchelaghem_h@yahoo.fr)

---

**Abstract.** Externally bonded reinforcement using Fiber Reinforced Polymer (FRP) is a good response to the concern represented by the need for rehabilitation of concrete structures. These techniques are more and more attractive because of their fast and low labour costs, very good strength to weight ratio, good fatigue properties, and non-corrosive characteristics of FRP. The present work is an experimental study investigating the mechanical behaviour under a uni-axial loading of short concrete columns reinforced by composite materials. These are constituted of glass fibers GFRP (bidirectional fabric of two surface densities 500 and 300 g/m<sup>2</sup>), carbon CFRP (unidirectional sheet of density per unit area of 230 g/m<sup>2</sup>) and polyester and epoxy resin respectively. The investigation aims at demonstrating the effectiveness of FRP reinforcement through highlighting the effect of thickness (FRP number of folds), the nature of the reinforcement (glass, carbon or Hybrid), and the orientation of the fibers. The axial lengths shortening along with the radial expansion are measured using the strain gauges glued to the outer surfaces of the composite jacket via a Wheatstone bridge. These measurements are saved to a PC through an acquisition card. The results obtained clearly show that the columns reinforced with CFRP folds allow an important increase in the compressive rupture stress in comparison with those reinforced with GFRP folds. The gains in compressive strength, in axial and in radial strains of the confined concrete with the different FRPs used are identified and quantified. It has further been demonstrated that the tested columns mechanisms depend strongly on the type of fiber reinforcements.

---

**Key words:** Concrete columns reinforcement; uni-axial compression; FRP; Structure rehabilitation; Fiber orientations.

### 1. Introduction

The durability of reinforced concrete structures depends on their behavior in relation to the climatic and environmental conditions that exist in the environments in which they are constructed. These structures are often exposed to numerous physico-chemical aggressions which they must satisfy, during their period of use, all the functions for which they were designed.

When they can no longer resist these aggressions, disorders appear in the concrete of these structures. These disorders are generally due to design flaws, poor implementation or accidental causes, but these disorders can be also due to non-compliance with quality standards in manufacturing by certain companies. These behaviors, if not rectified, undermine the durability, resistance and stability of the structures and can lead to their degradation and then their ruin (Ndzana Akongo, 2007).

Fiber-reinforced polymer (FRP) structural composite technology appeared for the first time in the mid-1930s as an experimental boat hull made of glass fiber and polyester resin. From military applications in the 1940s to the manufacturing and industrial sectors in the 1950s, FRP composites have gradually become the preferred alternative to traditional repair techniques.

Their popularity was mainly due to their excellent strength-to-weight ratio and their superior strength, inherent in climatic conditions and the corrosive effects of salt media (MAPEI, 2015). Numerous research and practical projects have demonstrated the effectiveness of the rehabilitation technique of buildings and structures by bonding FRP elements used as external reinforcement (Lam, 2009; Karbhari, 2009; Karbhari, 2004; Mirmiran, 1997).

An experimental and analytical study carried out by Tamuzs et al. (2007) on the deformability and concrete reinforcement by steel bars, compared with the properties of concrete specimens externally confined by FRP. They carried out experiments to estimate the participation of the steel bars reinforcement and the carbon/epoxy confinement of the concrete cylinders.

The effect of composite confinement architectures (E glass /Vinylester and carbon/epoxy) on the effectiveness of concrete columns reinforcement of the wrapped and then subjected to compression loading was investigated experimentally by Zhang et al. (2000). Moreover, these authors proposed evaluating the efficiency of each individual system by a cost index.

Shehata et al. (2002) carried out 54 tests on short columns to determine the strength and ductility gains of the concrete columns by covering them with carbon FRP sheets. Equations have been proposed to calculate the strength of the confined concrete and its ultimate specific deformation as a function of the lateral confinement stress.

The present work is an experimental investigation carried out on a series of cylindrical columns of concrete subjected to uni-axial compression. Two types of composite material confinement are used (GFRP and CFRP) and six stacks are made (see Table 1).

The aim of this study is to highlight the effectiveness of the reinforcement by FRP through the study of the influence of the envelope FRP staking sequence and the type of reinforcement (glass or carbon fiber) on the confined columns structural behavior. The strength, axial and radial strains gains are evaluated and analyzed, with identification of the failure and damage modes of the reinforced specimens.

**Table 1. Specimen's classifications.**

Description	Stack	Description	Stack
Concrete Pilot	not confined	T500	3tr_T500
C2	(0 <sub>2</sub> /90 <sub>2</sub> )	H1	2tr_H_t500 t300
C4	(90 <sub>2</sub> /0 <sub>2</sub> )	H2	2tr_H_t300 t500
		H3	2tr_H_T-Mat

## 2. Material study and experimental protocol

### 2.1. Concrete columns preparations

The concrete cylinders specimens having a size of 16 × 32 cm are prepared by a series of 50 samples by a company with a concrete plant (GESI-BAT, Algeria), thus obtaining the more or less uniform specimens. After 28 days, the surfaces of the concrete cylindrical specimens are brushed in order to obtain a rough and clean surface.

In other words, the purpose of the surface preparation of the concrete is to remove any surface traces of oil, grease, formwork and other soiling in order to achieve a clean surface able to receive the resin. The cylindrical surfaces ends are ground with a stone to ensure the flatness of the contact surfaces and their perpendicularity to the cylindrical one.

### 2.2. FRP external confinement

The technical adopted in this work for confining the specimens by FRP layers is the direct in-situ stratification technique. Two types of resins are used for two different reinforcements, the first one is a polyester resin used for both types of bi-directional fabrics (T500) and (T300) and the



Mat (M300) made of glass fibers (T, H1, H2 and H3). However, the second is SIKADUR 330 epoxy resin used for a SIKA WRAP HEX 230 C carbon fiber unidirectional sheet for C2 and C4 confinements (Fig. 1).



Fig 1. Different types of reinforcements used.

### 2.3. Compression test

In order to evaluate the behaviour of wrapped concrete columns a strain gauges are glued to the center of each specimen vertically and horizontally. These strain gauges measure axial shortening and radial expansion using a Wheatstone bridge. The specimens loading must be carried out without shock and continuously at a constant speed throughout the test.

### 2.4. Preparation of the polyester resin

The polyester resin used consists of three components (the resin, the hardener and the accelerator. Their preparation is easy, the desired quantity of the resin is put into a plastic bowl and then 1.5% of hardener is added and then mixed until a pink color is obtained, and finally 1 % of the accelerator is added and mixed again until the mixture becomes dark green, so the resin is ready to be used.

### 2.5. Preparation of the epoxy resin

The epoxy resin SIKADUR 330 consists of two components, resin and hardener (Fig. 2), which must be mixed shortly before application. The proportion by mass of the hardener represents 25% of the mass of the resin according to the recommendations of the supplier. The mixing is carried out for about three minutes until complete disappearance of the color streaks and obtaining a homogeneous mixture.



Fig 2. Components of the epoxy resin used.

### 2.6. Specimens FRP wrapping

Two types of reinforcement are used, Glass fiber reinforced polymer (GFRP), and CFRP (Carbon fiber reinforced polymer). The fabric reinforcing bands (glass or carbon fibers) were measured

and then cut with a cutter and a metal ruler. The length of the confinement bands fold correspond to the perimeter (for a layer) or to  $n$  times for  $n$  layers. In addition, the outer layer is extended (overlapping in the longitudinal direction of the fibers) in order to ensure a  $\frac{1}{4}$ -perimeter overlap which allows the full strength of the fibers to be developed without slipping or peeling the composite layer (Fig. 3).

The main advantage of dry fabric reinforcement is easy handling on site, without any heavy equipment to move. This technique allows in particular a perfect follow-up of the shape of the reinforced structure.



**Fig 3. Column wrapped models.**

## **2.7. Testing machine and instruments**

The simple compression tests were carried out with a constant loading speed until rupture in accordance with ASTM C39 / C39M-9a, using a hydraulic press with a capacity of 3000 kN "CONTROLS Model 50-C55G2/ " equipped with a DIGIMAX PLUS (Fig. 4). The data are transmitted to the automatic acquisition system via an interface. The tests are carried out within the Laboratory of Civil and Hydraulic Engineering (LGCH) of the University 08 May 1945 of Guelma.



**Fig 4. Testing machine and Wheatstone bridge.**

## **3. Results and discussions**

### **3.1. GFRP wrapped specimens effects**

The experimental tests results are graphically presented in the form of stress/strain curves in FIG. 5. The curves of the stresses are plotted as a function of the axial and radial strains in the

same reference frame. Typically, these curves have an initial slope which follows that of the control concrete up to a point of inflection, followed by a zone of great plastic deformation. While, the second slope in the plastic area is much lower than the first. This characterizes the contribution of the reinforcement which depends on the orientation and the nature of the fibers of the composite envelope.

The curves show the effect of the stacking sequence on the structural behavior of the confined specimens compared to that of the control concrete subjected to compression loading.

The analysis of the results obtained shows that the specimens wrapped by T500 or H3 gives an increase of 65 and 60% in the resistance respectively. Whereas, the hybrids H1 and H2 having the ultimate stresses equal to 39 and 37 MPa respectively, thus allowing an improvements of 43 and 41% respectively (Table 2).

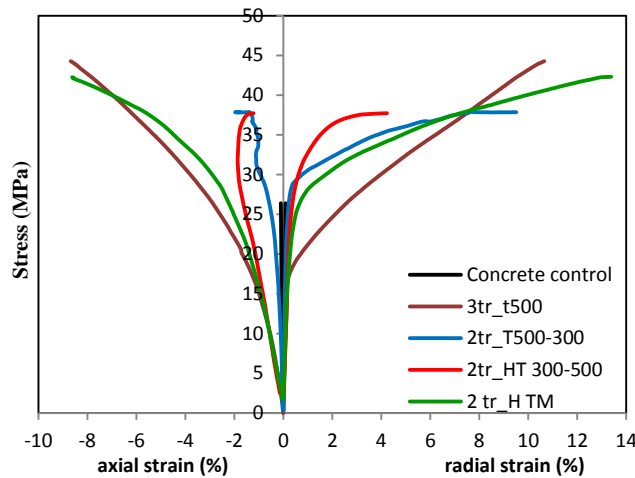


Fig 5. Stress/strain behavior of stacks in GFRP.

### 3.2. CFRP wrapped specimens effects

The mechanical behavior of columns confined by envelopes constituted by four CFRP plies having a stacking sequence of C2 ( $0_2/90_2$ ) and C4 ( $90_2/0_2$ ) are illustrated in Fig. 6. The confined columns are subjected to repetitive uniaxial compression loading until their final failure (i.e. until obtaining the load failure lower than the one of the control concrete).

The stress/strain curves of specimens wrapped by CFRP ( $0_2/90_2$ ) and ( $90_2/0_2$ ) respectively show that the C2 resists up to seven loads whereas, C4 resists only two loads (Figs. 6 and 7). The comparison of C2 and C4 for the first two loads showed bilinear behavior (Fig. 7). C2 lead to have the best ultimate load capacity at the second loading where the stress reached 61.41 MPa, i.e. an increase of 136% compared to the control concrete. However, C4 present the best behavior from the point of view of repetitive loading with a maximum stress of 49.9 MPa obtained during the third loading to an increase of 89 %.

The analysis of the C4 strains for the two loadings showed that the obtained axial and radial strains are practically identical and increase by (356%) and (1252%) respectively compared to the ones obtained for the control concrete. However, for C2, the axial and radial strains gains obtained are lower than those found for C4 and the both are equal to 23% (Table 2). In general, the two stacking sequences of the CFRP composite used for the confinement of the columns show a high performance compared to the GFRP composite studied. This is in good agreement with previous works of Bouchelaghem et al. (2011 a,b).

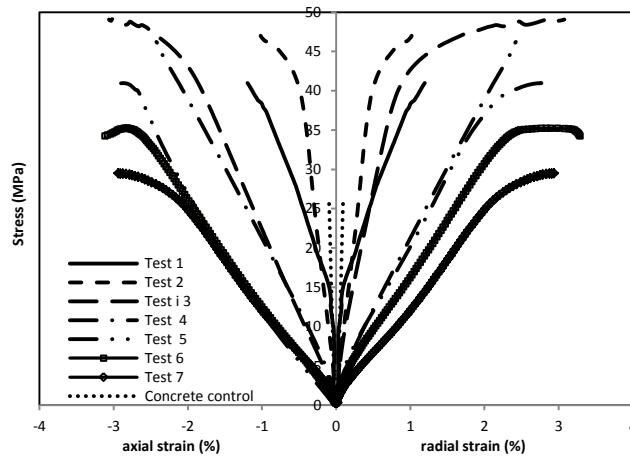


Fig 6. Stress/strain behavior of the repeated loading of the column wrapped by C2 (02/902).

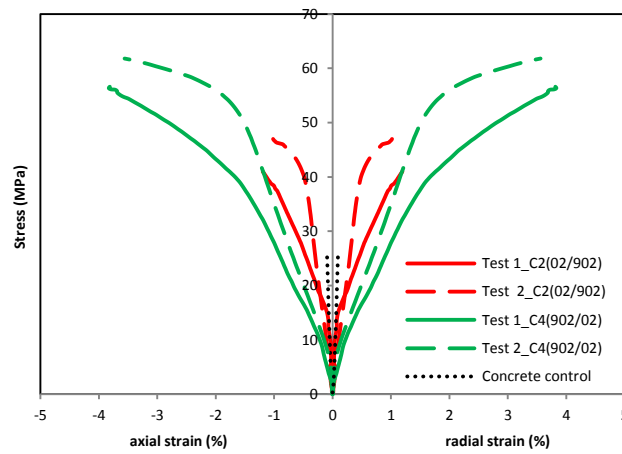


Fig 7. Comparison between the stress/strain behavior, first and second loading, of C2 (02/902) and C4 (902/02).

Table 2. Mean values of the test results of confined columns..

Config.de confin.	$F_{max}$ (kN)	$f'_c$ (MPa)	$f'_{cc}$ (MPa)	$f'_{cc}/f'_{co}$	$\epsilon_{cc}$ %	$\epsilon_{cc}/\epsilon_{co}$	$\epsilon_{r, rup}$ %	$\epsilon_{r, rup}/\epsilon_{ro}$
Concrete control	530.45	26.39	26.39	1.00	0.98	1.00	0.92	1.00
T	909.44		43.74	1.65	8.42	8.59	10.65	11.57
H1	759.27		37.83	1.43	1.74	1.77	8.75	9.51
H2	757.90		37.41	1.41	1.84	1.87	5.43	5.90
H3	858.72		42.30	1.60	8.21	8.37	13.39	14.55
C2	829.50		41.66	1.57	1.15	1.23	1.21	1.23
C4	1137.77		56.35	2.13	3.71	3.78	3.83	4.16

$f'_{cc}$ : axial compressive strength of confined concrete;  $\epsilon_{cc}$ ,  $\epsilon_{r, rup}$ : axial and radial deformations respectively.

### 3.3. Failure modes of the columns confined by CFRP and GFRP

The Fig. 8 shows the fractures of the specimens confined by GFRP and CFRP. In the case of GFRP the damage is initiated by local delaminations between the FRP envelope and the concrete which results in a change of color noted on the photos (the most damaged areas change its color and become white due to the delamination). Then, a crack growth is obtained in the directions of the fibers (horizontal and vertical), whereas the total failure of the composite jacket is obtained by a dominate crack which occur in the vertical direction (i.e. in the direction of loading).

The damage are located in the lower parts of the columns confined by the C4 (90<sub>2</sub>/0<sub>2</sub>) envelopes having the layer oriented at 0 in contact with the concrete. However, the cracks and breaks observed are located in the upper parts for the columns confined by C2 (0<sub>2</sub>/90<sub>2</sub>) envelopes having the layer oriented at 90 in contact with the concrete.

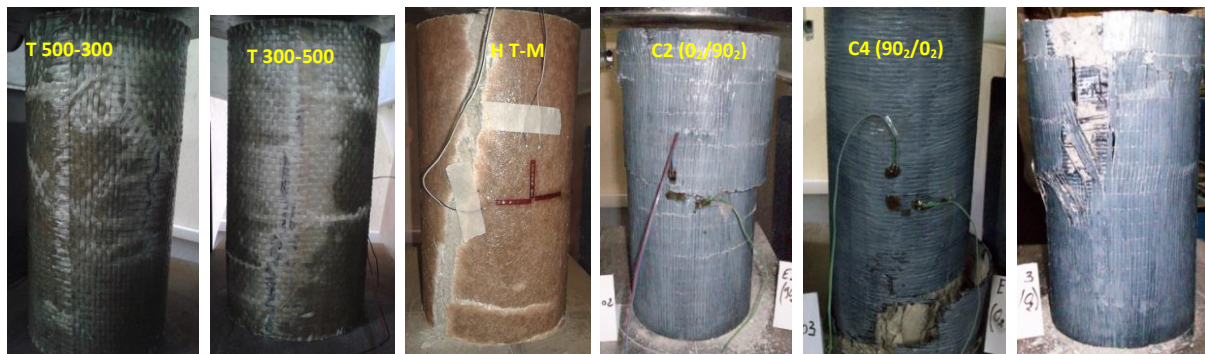


Fig 8. Failure facies of the columns confined by the envelopes: a) GFRP T500, H1, H2, H3 and control concrete, b) CFRP (0<sub>2</sub>/90<sub>2</sub>) and (90<sub>2</sub>/0<sub>2</sub>).

Columns confined by FRPC envelopes are generally characterized by fragile fracture obtained by explosion or brutal of the composite jacket; as is the case with stacking C4 (90<sub>2</sub>/0<sub>2</sub>) and (0<sub>2</sub>/90<sub>2</sub>). These phenomena are caused not only by the high strength of the carbon fibers but also by the rigid confinement due to a large number of folds (four plies) and their orientations. Indeed, the fibres oriented at 0 are subjected to the tensile loading due to swelling of the test specimens during loading, while, the one oriented at 90 are loaded at compression.

The use of GFRP composite materials in the repair and/or reinforcement of concrete structural elements (short columns), subjected to uni-axial compression have an acceptable efficiency in strength, axial and radial strains compared to those confined by CFRP. The Fig. 9 clarifies the effectiveness of this technique and shows well the gains and increases obtained for each system.

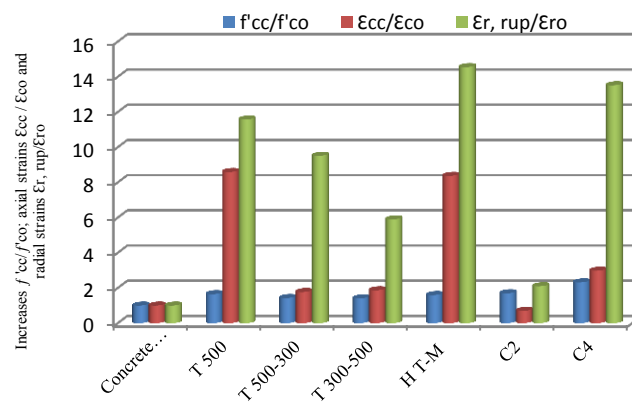


Fig. 9. Effectiveness of concrete reinforcement by FRP in terms of stresses axial and radial strains.

## 4. Conclusions

According to the study of externally wrapped concrete columns subjected to uni-axial compression loading the main conclusions are:

- The columns confined by the GFRP and CFRP composite subjected to a repetitive loadings, showed a more rigid compared to the concrete control;
- The best gains in axial and radial strains are equal to 356% and 1252% respectively obtained for the column wrapped by C4 (90<sub>2</sub>/0<sub>2</sub>). While, for C2 (0<sub>2</sub>/90<sub>2</sub>), the axial and radial strains gains obtained are for the both only 23%;
- The study of the columns confined by the hybrids adopted H1, H2 and H3 showed that their stress/strain behaviors follow the first folds i.e. the layers in direct contact with the concrete; however, their failure mode damage types follow the one of the external folds;
- Fractures of columns confined by CFRPs are marked by a brutal rupture of carbon fibers.

## 5. References

- Bouchelaghem, H., Bezazi, A., & Scarpa, F. (2011). Compressive behaviour of concrete cylindrical FRP-confined columns subjected to a new sequential loading technique, *composite parte B*, 42, 1987-1993.
- Bouchelaghem, H., Bezazi, A., & Scarpa, F. (2011). Strength of concrete columns externally wrapped with composites under compressive static loading, *Reinforced Plastics and Composites*, 30 (19), 1671-1688.
- Karbhari, V. M. (2004). Fiber reinforced composite bridge systems–transition from the laboratory to the field, *Composite Structures*, 66, 5-16.
- Karbhari, V. M., & Ghosh, K. (2009). Comparative durability evaluation of ambient temperature cured externally bonded CFRP and GFRP composite systems for repair of bridges, *Composite: Part A*, 40, 1353-1363.
- Lam, L., & Teng, J.G. (2003). Design-oriented stress–strain model for FRP-confined concrete, *Construction and Building Materials*, 17, 471-489.
- MAPEI (2015). Corporation, Polymères renforcés de fibres (PRF), Siège social des Amériques.
- Mirmiran, A., & Shahawy M. (1997). Dilation characteristics of confined concrete, *mechanics of cohesive frictional Materials*, 2, 237-249.
- Ndzana Akongo, & Tchoumi, S. (2007). Réhabilitation des ouvrages en béton armé dégradés par la corrosion des armatures, Université de Douala.
- Shehata, L A. E. M., Carneiro, L. A. V., & Shehata, L. C. D. (2002). Strength of short concrete columns confined with CFRP sheets, *Materials and Structures*, 35, 50-58.
- Tamuzs, V., Valdmanis, V., Gylltoft, K., & Tepfers, R., (2007). Behavior of CFRP-confined concrete cylinders with a compressive steel reinforcement, *Mechanics of Composite Materials* 43 (3).
- Zhang, S. L., Mai, Ye Y.W. (2000). A Study on Polymer Composite Strengthening Systems for Concrete Columns, *Applied Composite Materials*, 7, 125-138.

## Mechanical strengths of modified PET mortar composites in aggressive $MgSO_4$ medium: ACI & B.S predictions

Kazi Tani N<sup>1,4\*</sup>, Benosman A.S.<sup>1,2,3</sup>, Senhadji Y.<sup>3,5</sup>, Taïbi H.<sup>2</sup>, Mouli M.<sup>3</sup>

- 1 Higher School of Applied Sciences (ESSA-T), BP 165, 13000 Bel Horizon, Tlemcen, Algeria.
  - 2 Faculty of Exact and Applied Sciences, Laboratory of Polymer Chemistry LCP, University of Oran 1, Oran, Algeria.
  - 3 Department of Civil Engineering, LABMAT, ENPO Maurice Audin, Oran, Algeria.
  - 4\* LCGE Laboratory, Faculty of Mechanical Engineering, USTO-MB, Oran, Algeria.
  - 5 Department of Civil Engineering, University of Mustapha Stambouli, Mascara, Algeria.
- \* Corresponding Author: [kazitani\\_nabil@yahoo.fr](mailto:kazitani_nabil@yahoo.fr)

---

**Abstract.** Composites mortars based on plastic aggregates are often considered as an innovative materials of the future because of their potential and the advantages they present. In this paper, a comparative study was carried out on the effect of magnesium sulfate  $MgSO_4$  (5%) attack on the durability of composite mortars modified by recycled polyethylene terephthalate (PET). Laboratory tests were accomplished on limestone sand and cement mortars where the blended Portland cement was partially replaced by various volume fractions of PET plastic aggregates. Mechanical properties measured on specimens were used to assess the changes in the compressive strengths of PET-mortar composites exposed to  $MgSO_4$  attack at different ages, mainly the Young modulus of elasticity. Based on experimental compressive tests on selected specimens and their densities, the evolution of static Young modulus of elasticity has been discussed in accordance to predicted models proposed by (ACI-318) and (BS-8110) codes of practice. In addition, a comparative analysis has been carried out for corrosion resistance coefficients  $K$  of referenced mortar to those modified with plastic aggregates. It can be noted that, the corrosion resistance coefficients decrease as much as composite specimens are exposed to  $MgSO_4$  corrosive medium. For the case of modified composites, the values of  $K$  based on predicted Young modulus before and after immersion are better than the ones calculated for the unmodified mortar. Therefore, ACI 318 prediction model is recommended code for design and investigation works related to repair mortars, screeds, pavements...etc. Also, it can be concluded that adding PET plastic aggregates by volume to blend Portland cement act to improve the corrosive resistance of this cement against  $MgSO_4$  aggressive medium.

---

**Key words:** Recycled polymer aggregates, Composite mortars,  $MgSO_4$  Solutions, Mechanical properties, Sustainable materials.

### 1. Introduction

In the recent previous decades, polyethylene terephthalate (PET) is produced within large amount in industrial countries (planetoscope, html) and since waste PET is not biodegradable, then, it can remain in nature for hundreds of years and causes too many ecological problems.

Several research works were carried out recently by too many authors in the field of material science applied to building industries, such as (Alfahdawi et al. 2016; Benosman, 2013; Gu and Ozbakkaloglu, 2016; Rahmani et al. 2013; Sharma and Bansal, 2016) in order to find ecologic and green ways to dispose and recycle polymer wastes.

One of the main proposed technics by researchers is to introduce PET in the technology construction materials by substituting volumetric amount of cement (Benosman et al. 2017a) and/or aggregates (Azhdarpour et al. 2016; Hannawi et al. 2010; Zuccheratte et al. 2017) in concrete and mortars mix-design.

In this paper, the influence of magnesium sulfate attack on the durability of composites produced with waste polyethylene terephthalate (PET) is studied. Experiments were accomplished on cement mortars and limestone sand where the blended Portland cement was partially replaced by various volumetric fractions of PET particles (6%, 12% and 17%<sup>v</sup>).

Test solution used to provide the sulfate attack was 5% of MgSO<sub>4</sub> solution. Tap water was used as the control medium. Compressive strengths measured on specimens were used to assess the changes in the mechanical properties of modified mortars subjected to MgSO<sub>4</sub> attack at different ages, mainly the Young modulus of elasticity.

## 2. Raw materials

### 2.1. Cement

The cement used was a blended Portland cement type CPJ-CEM II/A42.5 supplied by Zahana factory, located in western Algeria, with 1022 kg/m<sup>3</sup> bulk density; its compressive strength at 28 days was 42.5 MPa. The absolute density of the cement used was 3.15 g/cm<sup>3</sup> and its specific surface area measured with the Blaine method was 3532 cm<sup>2</sup>/g. Its initial and final setting times were 170 and 245 min, respectively. Mineralogical and chemical compositions of cement are listed in Table 1. The chemical composition was obtained using an X-ray fluorescence spectrometer.

**Table 1. The chemical and mineralogical compositions of cement (wt.%)**

Chemical compositions	SiO <sub>2</sub>	20.91
	Al <sub>2</sub> O <sub>3</sub>	5.52
	Fe <sub>2</sub> O <sub>3</sub>	3.56
	CaO	63.50
	MgO	0.64
	SO <sub>3</sub>	2.79
	K <sub>2</sub> O	1.23
	Na <sub>2</sub> O	0.13
	CaO free	2.35
LOI	1.19	
Mineralogical compositions	C <sub>3</sub> S	49.39
	C <sub>2</sub> S	22.97
	C <sub>3</sub> A	8.61
	C <sub>4</sub> AF	10.83

### 2.2. Sand

The crushed natural limestone sand was obtained from the quarry of Kristel, in Oran, West Algeria. The maximum size of sand grains was 5 mm. The absolute density and absorption coefficient of crushed sand were 2.53 g/cm<sup>3</sup> and 0.5%, respectively. The grading of crushed sand is presented in Table 2, according to standard NF P18-560 (AFNOR, 1990).

### 2.3. Waste Polyethylene Terephthalate

Waste PET bottle granules (PET) used as particles were supplied by TRAMAPLAST PET Bottle Plant, in Tlemcen, Algeria. These particles were obtained by collecting the waste PET bottles and washing them; they are then crushed by granules into machines. In addition, they have an irregular shape and a rough texture surface, which enables the adherence of the particle-matrix. The bulk density of the WPET particles used was 401.4 kg/m<sup>3</sup>.



After preliminary tests, PET particles of size lower than 1 mm were used in this study. The sieve analysis of PET particles was carried out according to standard NF P18-560 (AFNOR, 1990) and is presented in Table 2.

**Table 2. The sieve analysis of waste PET-Particles and crushed limestone sand**

Sieve size (mm)	Cumulative passing (%)	
	PET	Sand
5	99.92	99.83
2.5	98.16	98.37
1.25	96.82	65.37
0.63	55.78	38.3
0.315	35.48	19.07
0.16	18.28	8.20
0.125	9.56	3.325

### 3. Composite mixing conditions

The mortar manufactured without WPET particles was first optimized on the basis of its mechanical criteria and was then used as a reference composite. The composites containing PET particles were produced in accordance with the results of the works of Benosman et al. (2017b). A massic ratio of 3 between sand (S) and cement (C) was respected. Four different mixtures were prepared (the control mixtures without plastic waste and three PET# mixtures including 6%, 12% and 17% waste PET particles by volume). Mixture name of the different composites were: PET0 (without plastic waste), PET6, PET12 and PET17. The water to binder ratio was kept constant at 0.5. So, after pouring fresh material into the molds (EN 196-1, 2005), the samples were stored in a room where hygrometry and temperature were controlled for 24 h (98% relative humidity, and  $20 \pm 1$  °C). After removal from the molds, at 1 day of age, mortar specimens were cured in saturated lime water at  $20 \pm 1$  °C, until the time of testing.

### 4. Test methods of resistance to $MgSO_4$ attack

The mortar specimens were cured in water saturated with lime at  $20 \pm 1$  °C for 28 days before being exposed to sulfate attack. Three specimens of each mortar and composite mixes ( $40 \times 40 \times 160$  mm<sup>3</sup>) were immersed in two types of solutions: fresh water (reference medium) and 5% magnesium sulfate ( $MgSO_4$ ), Figure 1. According to the standard ASTM C1012-04 (2004), the pH of the sulfate solution should be between 6 and 8 and the solution must be renewed each week, which requires huge amounts of magnesium sulfate.



**Fig 1. Immersion of the specimens in the aggressive solution**

For this, Mehta's method (1975) and that of Siad et al. (2013) were adopted; they all recommend the control of the pH within a range of 6.0–8.0 by adding a suitable amount of sulfuric acid solution (0.1N  $H_2SO_4$ ), Figure 2. The correction is performed daily during the first weeks of

immersion, and then becomes weekly, for the rest of the test. In addition, the aggressive solutions were totally renewed each 12 weeks. After immersion in magnesium sulfate solution ( $\text{MgSO}_4$ ) for the required period of time, ASTM C1012-04 (2004), the specimens were tested for residual mechanical properties. The Young modulus loss (YML%) is calculated as follows:

$$YML(\%) = \frac{E_{cr} - E_{cs}}{E_{cr}} \times 100 \quad (1)$$

Where  $E_{cr}$  is the Young modulus of the specimens before immersion (MPa) and  $E_{cs}$  is the average Young modulus of the specimens after immersion in magnesium sulfate solutions for the required period of time (180 days).



Fig 2. Correction of the sulfate solution by adding small quantities of 0.1N  $\text{H}_2\text{SO}_4$ , up to a pH equal to 6-8.

## 5. Results and discussion

### 5.1. Prediction models of Mechanical Properties

The static modulus of elasticity  $E$  (Young Modulus) represents the one of the most important mechanical characteristics of construction materials (Concrete, Reinforced concrete, mortars, composites ...etc). This intrinsic property is considering as the basic parameter for the computing strain-stresses in construction structures. Various countries have been established their design codes based on this empirical relationship between static modulus of elasticity  $E$ , and compressive strength of plain concrete at 28 days of curing. The ACI code (ACI-318, 2005) defines the relationship between elastic modulus of concrete and compressive strength as:

$$E_c = w^{1.5} 0.0043 f^{0.5} \quad (2)$$

The British Code of practice (BS-8110, 1997) recommends the following expression for static modulus of elasticity with cube compressive strength of concrete as:

$$E_c = w^2 0.0017 f_c^{0.33} \quad (3)$$

Where,  $E_c$  represents the static modulus of elasticity at 28 days in MPa

$f_c$  : Compressive strength at 28 days in MPa

$w$  : Air dry density of mortar

Based on experimental compressive tests on PET-Mortar composite specimens (Benosman et al. 2013), and there densities, graphs in (Figures 3, 4) bellow show the evolution of Young modulus evaluated by empirical relationships in accordance to (ACI-318) and (BS-8110) codes.

The results of the Young modulus loss using the specimens immersed in 5%  $\text{MgSO}_4$  solutions (Figure 5) showed that there are variations in time and group. However, a decrease in Young Modulus values of all specimens was observed when Young Modulus of elasticity is computed

via ACI-318 model. It was expected that the mechanical properties loss (YML%) values of modified mortars with PET plastic particles would be lower than those of unmodified mortar PET0, by 16.84%, 21.35% and 18.40% for PET6, PET12 and PET17, respectively for the case where the prediction model is BS-8110 and respectively by 12.00%, 18.30% and 13.40% when Young Modulus of elasticity is computed via ACI-318 model. It can therefore be concluded that modified mortars by PET plastic particles are resistant to the magnesium sulfate aggressive exposure conditions often encountered in the field.

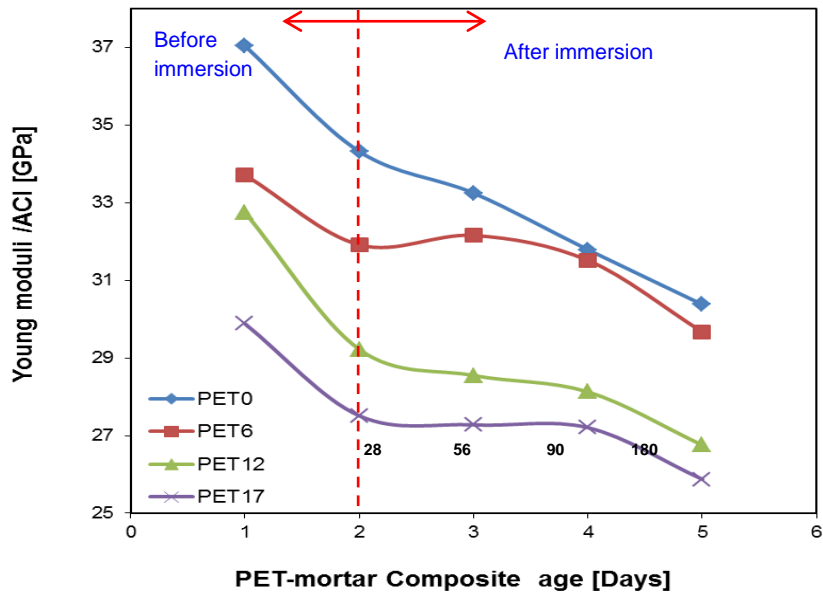


Fig 3. Evolution of Young modulus with volumetric PET rate and composite mortar ages via ACI-318 code before and after MgSO<sub>4</sub> attacks

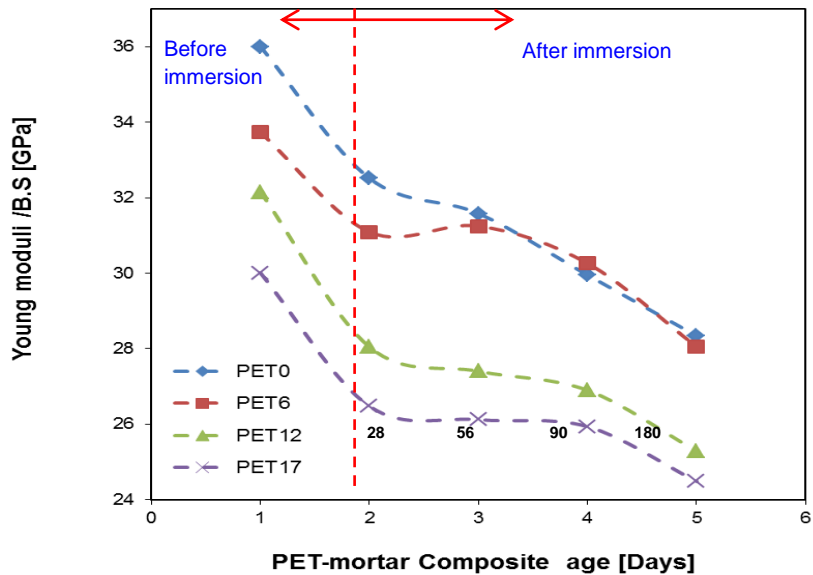


Fig 4. Evolution of Young modulus with volumetric PET rate and composite mortar ages via BS-8110 code before and after MgSO<sub>4</sub> attacks

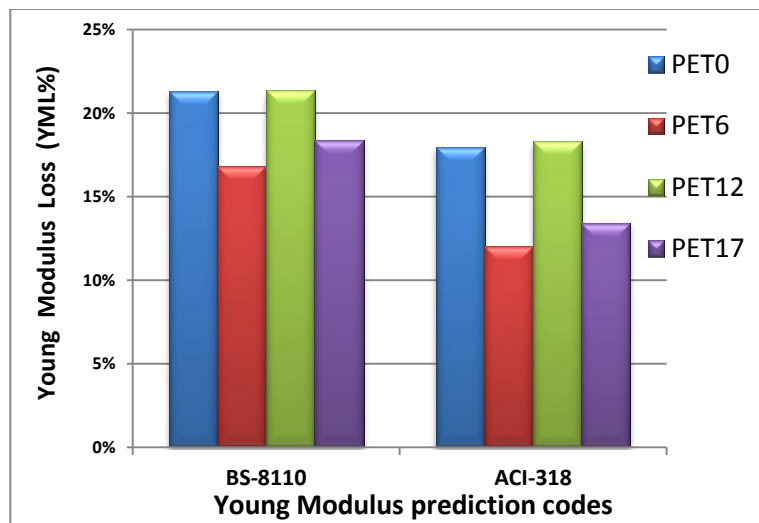


Fig 5. Young modulus loss (YML%) with volumetric PET rate and prediction codes (BS-8110 & ACI-318) before and after  $MgSO_4$  immersion

### 5.2. Corrosion magnesium sulfate resistance

Furthermore, to compare, effectively, the corrosion resistance coefficients  $K$  of unmodified mortar (Eq. 4) to those modified with PET particles, as it was used by Benosman et al. (2017b) and Jiang et al. (2004):

$$K = E_{ci} / E_{cs} \quad (4)$$

Where  $E_{ci}$  is the Young modulus of composite mortars immersed in corrosive magnesium sulfate solutions,  $E_{cs}$  the Young modulus of the normally cured composite mortars.

The corrosion resistance coefficients of the specimens with and without PET plastic are given in Table 3. It can be seen from Table 3 that, for the composite immersed in a corrosive  $MgSO_4$  solution, the corrosion resistance coefficients decrease with the increase of the immersion period. The corrosion sulfate resistance  $K$  based on Young modulus before and after immersion of PET-mortar composites is better than that of the control mortar (PET0).

Table 3. The corrosion resistance coefficients of PET-mortar composites in 5%  $MgSO_4$

$MgSO_4$ Attacks	K (BS.8110)		K (ACI.318)	
	90 Days	180 Days	90 days	180 Days
PET0	0.832	0.787	0.858	0.820
PET6	0.897	0.832	0.935	0.880
PET12	0.836	0.786	0.859	0.817
PET17	0.864	0.816	0.910	0.866

For all studied cases, corrosion resistance coefficients  $K$  computed via ACI 318 are slightly higher than the ones evaluated by BS.8118 code of practice. Therefore, in order to obtain a safe design using PET-Modified mortar, ACI 318 is the recommended code for design and investigation Issues. Also, it can be concluded that adding PET by volume fractions to blended Portland cement renders this cement more resistant to the magnesium sulfate aggressive medium. (Miletic, 1999) reported that the resistance of cement to sulfate aggression is also related to its content in  $C_3A$ .

Consequently, using PET as cement substitutes reduces the energy consumption, contributes to save natural environment by reducing CO<sub>2</sub> emissions and is used to repair various reinforced concrete structures in magnesium sulfatic aggressive mediums.

Finally, the obtained results are in accordance with the ones reported by Alqahtani et al. (2017) which stated that recovering plastic waste would reduce the CO<sub>2</sub> emissions by 3.8 million tons. The advantages of durability properties of modified mortar exposed to MgSO<sub>4</sub> attacks indicate longer life of the repaired structures by using this type of green composite repair materials.

## 6. Conclusions

The main conclusions based on results plotted above, can be drawn as follows:

- PET-Mortar composites present a better behavior against aggressive medium such as magnesium sulfatic (MgSO<sub>4</sub>) and it reduces significantly the consumption energy related to CO<sub>2</sub> emission.
- In MgSO<sub>4</sub> corrosive medium, unmodified mortar (PET0) and substitution volumetric rate of PET act to decrease the mechanical properties of PET-Mortar composites, mainly, the static modulus of elasticity (computed by ACI-318 and BS-8110 codes). In addition, Prediction model proposed by ACI-318 gives always the lowest values of elastic Young modulus which can be recommended for structural design issues.
- The loss in static Young modulus of elasticity (YML%) of modified mortars are lower than the ones of unmodified mortars. The optimal minimal values of (YML%) are given by ACI-318 code of practice, mainly, for the case of PET-Modified mortars within volumetric rate of 6%, 17%. The corrosion resistance coefficients K decrease with exposure time to MgSO<sub>4</sub> aggressive medium.

**Acknowledgements** - The authors acknowledge financial support from the Ministry of Higher Education and Scientific Research of Algeria, under the grants CNEPRU B00L01UN310120130068.

## 7. References

- ACI 318. (2005). Building Code Requirements for Structural Concrete (ACI 318-05) and Commentary (ACI 318R-05), ACI Committee 318, American Concrete Institute, Farmington Hills, MI.
- AFNOR, (1990). Granulats. Analyse Granulométrique par Tamisage.. NFP 18-560, Association française de normalisation.
- Alfahdawi, I.H., Osman, S.A., Hamid, R., Al-Hadithi, A.I. (2016). Utilizing waste plastic polypropylene and polyethylene terephthalate as alternative aggregates to produce lightweight concrete: a review, *Journal of Engineering Science and Technology*, 11(8), 1165-1173.
- Alqahtani, F.K., Iqbal Khan, M., Ghataora, G., & Dirar, S. (2017). Production of recycled plastic aggregates and its utilization in concrete, *Journal of Materials in Civil Engineering*, ASCE, 04016248, 29(4), 1.
- ASTM C1012-04. (2004). Standard Test Method for Length Change of Hydraulic-Cement Mortars Exposed to a Sulfate Solution, C1012-04, Annual Book of ASTM Standards.
- Azhdarpour, A.M., Nikoudel, M., & Taheri, M., (2016). The effect of using polyethylene terephthalate particles on physical and strength-related properties of concrete; a laboratory evaluation, *Construction and Building Materials*, 109, 55-62.
- Benosman, A.S. (2013). Performances, Propriétés Thermiques et Durabilité des Composites Mortier-Polytéréphtalate d'éthylène PET, Dossier d'Habilitation Universitaire, Université Abou-Bekr Belkaid, Tlemcen.
- Benosman, A.S., Mouli, M., Taibi, H., Belbachir, M., Senhadji, Y., Bahlouli, I., & Houivet, D. (2013). La Durabilité des Matériaux Composites PET-Mortier dans un Environnements Agressifs, In the

- 
- proceedings of CIMDD'2013, ISBN : 978-9931-9090-1-9, Université Boumerdès, Algérie, 06-09 Mai 2013, 330.
- Benosman, A.S., Mouli, M., Taïbi, H., Belbachir, M., Senhadji, Y., Bahlouli, I., & Houivet, D. (2017a). The Chemical, Mechanical and Thermal Properties of PET-Mortar Composites Containing Waste PET, *Environmental Engineering and Management Journal*, 16 (7), 1489-1505.
- Benosman, A.S., Taïbi, H., Senhadji, Y., Mouli, M., Belbachir, M., Bahlouli, M.I. (2017b). Plastic waste particles in mortar composites: sulfate resistance and thermal coefficients, *Progress in Rubber Plastics and Recycling Technology Journal*, 33(3), 171-202.
- BS 8110. (1997). Structural use of concrete. Code of practice for design and construction. British Standards Institution.
- EN 196-1. (2005). Methods of testing cement - Part 1: determination of strength, European Committee for Standardization, CEN.
- Gu, L., Ozbakkaloglu, T. (2016). Use of recycled plastics in concrete: A critical review, *Waste Management*, 51, 19-42.
- Hannawi, K., Prince, W. & Kamali-Bernard, S. (2010). Effect of thermoplastic aggregates incorporation on physical, mechanical and transfer behaviour of cementitious materials, *Waste Biomass Valorization*, 1, 251-259.
- <http://www.planetoscope.com/petrole/989-production-mondiale-de-plastique.html>
- Jiang, L., Liu, Z., & Ye, Y. (2004). Durability of concrete incorporating large volumes of low-quality fly ash, *Cement and Concrete Research*, 34, 1467-1469.
- Mehta, PK. (1975). Evaluation of sulfate resisting cements by a new test method, *Journal of American Concrete Institute*, 72(40), p 573-575.
- Miletić, S., Ilić, M., Otović, S., Folić, R., Ivanov, Y. (1999). Phase composition changes due to ammonium-sulphate: Attack on portland and portland fly ash cements, *Construction and Building Materials*, 13(3), 117-127.
- Rahmani, E., Dehestani, M., Beygi, M.H.A., Allahyari, H., & Nikbin, I.M. (2013). On the mechanical properties of concrete containing waste PET particles, *Construction and Building Materials*, 47, 1302 -1308.
- Sharma, R. & Bansal P.P. (2016). Use of different forms of waste plastic in concrete – a review, *Journal of Cleaner Production*, 112, 473-482.
- Siad, H., Kamali-Bernard, S., Mesbah, H.A., Escadeillas, G., Mouli, M., & Khelafi, H. (2013). Characterization of the degradation of self-compacting concretes in sodium sulfate environment: Influence of different mineral admixtures, *Construction and Building Materials*, 47, 1188-1200.
- Zuccheratte, A.C.V., Freire, C.B., & Lameiras, F.S. (2017). Synthetic gravel for concrete obtained from sandy iron ore tailing and recycled polyethyltherephthalate, *Construction and Building Materials*, 151, 859-865.
-

## Repair of reinforced concrete beams in shear using composite materials PRFG subjected to cyclic loading

Boumaaza M <sup>1,\*</sup>, Bezazi A <sup>2</sup>, Bouchelaghem H <sup>2,3</sup>, Benzannache N <sup>1</sup>, Amziane S <sup>4</sup>, Scarpa F <sup>5</sup>

1\* Laboratory of Civil Engineering & Hydraulics (LGCH)/Guelma University, Algeria

2 Laboratory of Applied Mechanics of New Materials ((LMANM)/University of Guelma, Algeria

3 Department of Mechanical Engineering/University of Constantine1, Algeria

4 Department of Civil Engineering, Polytech Clermont Ferrand/Blaise Pascal University, France

5 Advanced Composites Center for Innovation and Science (CCCTB)/University of Bristol, UK

\* Corresponding author: [messaoudabeb@yahoo.fr](mailto:messaoudabeb@yahoo.fr)

---

**Abstract.** Nowadays, finding new approaches to attenuate the effects of the catastrophic shear failure mode for reinforced concrete beams is a major challenge. Generally the bending failure is ductile. It allows a redistribution of the stresses providing an early warning, whereas the rupture by shear is fragile and sudden which can lead to detrimental consequences for the structures. This research focuses on the repair of deep beams in reinforced concrete shear subjected to 4-point bending. After being preloaded at different levels of their ultimate loads, the beams are repaired by bonding a composite material made of an epoxy resin reinforced by glass fibers. The main objective of this study is to contribute to the mastery of a new method developed by the authors that consists by banding the cracks in critical zones in order to avoid fragile ruptures due to the shear force. This new technique led to better results in terms of mechanical properties when compared to conventional methods, notably the absence of the debonding of the composite found in the case of the repairs of the beams by bands or U-shaped composites. The feasibility, the performances and the behavior of the beams have been examined. The experimental approach adopted using this new technique has shown the influence of the type of loading on the fatigue behavior. In addition, the repair performed led to a considerable improvement in the fatigue durability of the preloaded beam.

---

**Key words:** Deep beam, Shear failure, Preloading, Composite, Repair.

### 1. Introduction

During their lifetime, concrete structures can be subjected to different types of loading and environmental conditions. Cracks produced and preload conditions are initial damage that can affect long-term structural behavior. These initial cracks and damage propagate and increase over time as a result of cyclic loading. In the case of deep bridge beams, for example, the structural elements are subjected in service to maximum values stresses of generally known but time-varying, most of which result from cyclic variations in stresses.

Generally a bridge is designed for a century, even in a regulatory way, their operating conditions turns out to change following the development not only of the size and load of vehicles but also road traffic. This leads to a reduction in their initial lifetime, sometimes causing catastrophic ruptures even when they are subjected to cyclic of modest maximum value stresses. The phenomenon involved in this is fatigue damage. It is characterized by irreversible deformations in the form of cracks that develop slowly over time without macroscopic signs. By accumulating, these can lead to a catastrophic rupture.

Indeed, the literature review shows clearly that experimental research and analytical studies on the fatigue behavior of reinforced concrete (RC) beams reinforced or repaired with FRP are very limited. The majority of these studies relate to flexural reinforcement, while very few studies have been carried out on shear reinforcement (deep beams).

Meier et al. (1992) tested two RC beams reinforced with a hybrid glass/carbon composite. Bames and Mays (1999) conducted an experimental program to study the flexural behavior of reinforced RC beams using FRP under fatigue stress. The reinforcement used is a unidirectional composite fabric based on carbon fibers (CFRP) bonded to the underside of the beam (tensile zone), which leads to the conclusion that the internal reinforcement rate affects the failure mode. Shahawy and Beitelman (1999) tested six beams of T shape under cyclic fatigue with a loading level between 0 to 25% of the ultimate load.

Papakonstantinou et al. (2001) also conducted fatigue tests in 4-point bending at a frequency of 2 or 3 Hz on 14 reinforced RC, eight reinforced with glass fiber (GFRP), and six non-reinforced with different fatigue loading levels. On the one hand, they found that the fatigue failure of the reinforced beams is caused by the fatigue failure of the tensile steel armature reinforcements after their plastification and, on the other hand, the use of the FRP increases the lifetime of the beams loaded at cyclic loading.

Masoud et al. (2001) also performed fatigue tests under 4-point bending with a frequency of 3 Hz on RC beams, whose tensile steel armature are corroded, reinforced with a carbon fabric. The loading level is between 10% and 80% of the ultimate strength of unreinforced RC beams. The fatigue failure of reinforced beams is caused by the fatigue of the tensile armatures similarly to Shahawy and Beitelman (1999).

In addition, some studies have also investigated a structural elements preloaded, reinforcement with composite materials in particular (Arduini, 1997; Choi et al.; De Lorenzis and Teng, 2007; Boussaha, 2008; Kreit, 2011; Dong, 2013 and Teo, 2017). The problems of premature failure associated with the complexity and incomprehension of the shear behavior of RC beams, under cyclic fatigue loading (loading/unloading) were the aim of this study.

The main objective of this study is to elucidate, using an experimental investigations, the fatigue behavior of deep beams repaired by FRP using a new technique. This technique was developed recently by the authors Boumaaza et al. (2017) for static tests (non-cyclic). The deep beam, used in the present work, is tested under 4-point bending assuming that the shear failure mode is predominant, with cyclic loading. For this purpose, a beam is preloaded at 80% of its ultimate load and then it has repaired by composite materials using the new technique SCR. After at list 15 days, resin polymerization time, the beam is cycled 19 times at 65 % of its ultimate load.

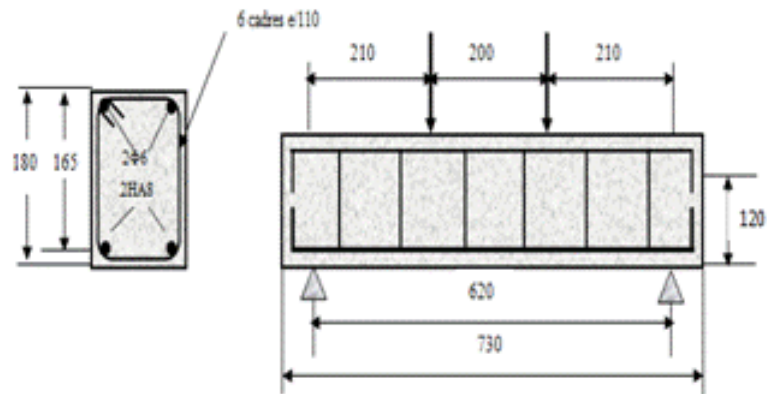
## 2. Experimental protocol

The aim of the experimental part is to investigate the fatigue behavior of the RC deep beams under cyclic loading (load/unload), repaired by glass fiber composites (GFRP) using the SCR technique. The concrete beams were designed in accordance with ASTM C78-00, armed with two HA8 in tensile zone and two HA6 in compressed zone, and 6 frames used as transverse reinforcements spaced of 110 mm. Fig. 1 shows the detail of the reinforcement in steel armatures of the beams. After at least 28 days, the manufactured beam is preloaded at 60% of its ultimate load.

The beam is repaired using the SCR technique which requires the preliminary work as follows:

- Drilling the beam on each side at the vicinity of the diagonal cracks of the concrete by passing through it (Figure 2a);
- Before the glass fabric was inserted, a repair was carried out using the mortar Fig. 2(b);
- The positions of the grooves, having 25 mm wide and 3 mm depth, were traced on the surface of the beam (Figure 2c). Then the grooves are subsequently cleaned of dust and concrete debris;

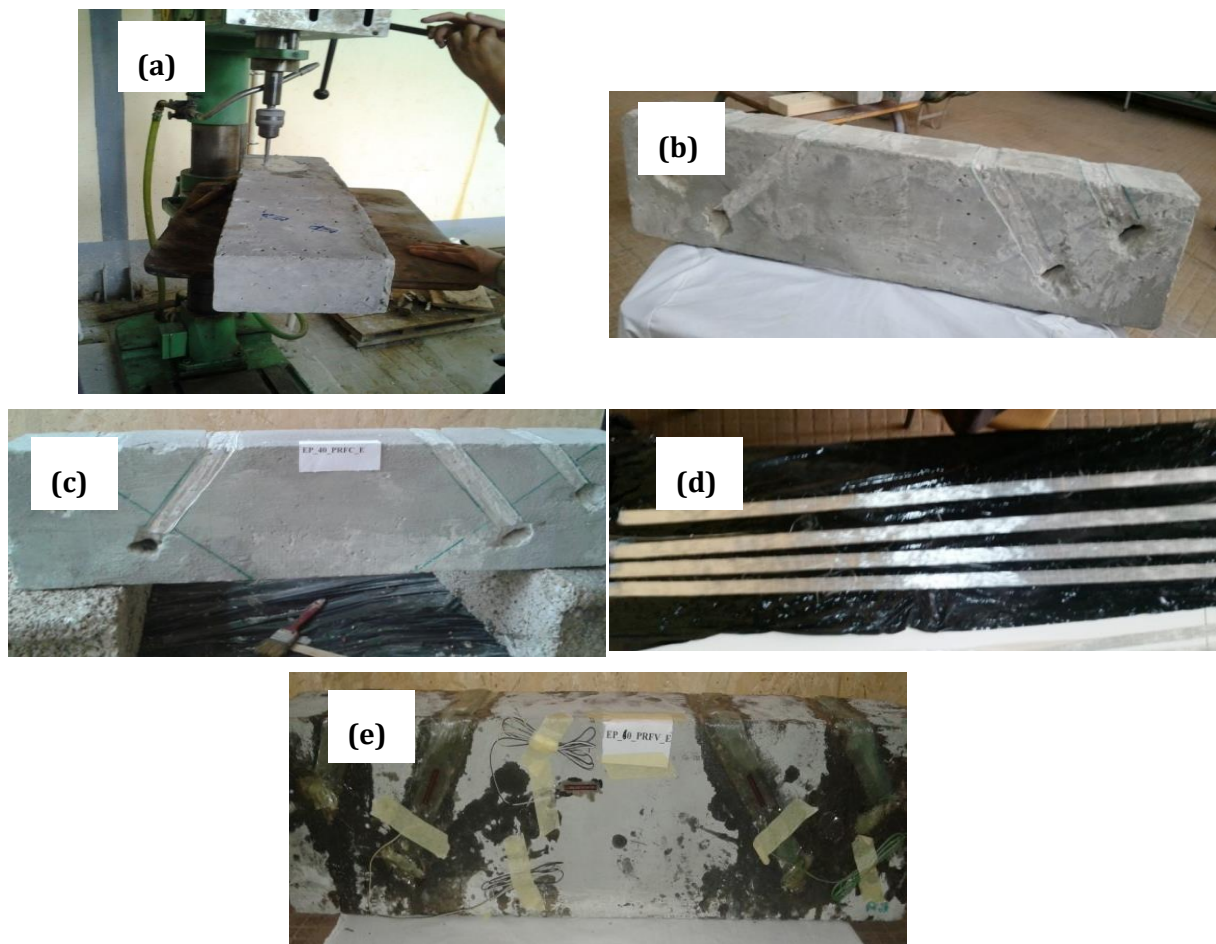




**Fig 1. Schematic layout of the specimen and steel reinforcement in accordance with ASTM 78-00.**

- The unidirectional of  $600 \text{ g/m}^2$  surface density fabric is cut in pieces having a size of  $1500 \times 25 \text{ mm}$  and  $1000 \times 25 \text{ mm}$ . Then the fabric, previously impregnated with the epoxy resin, is inserted into the grooves.

SCR repair involves introducing composite bands into holes in the shear zone in order to band the diagonal cracks (Figure 2d).



**Fig 2. Repair of the beam (a) drilling of the holes (b) grooving (c) mortar reparation (d) cut of the unidirectional fabric (e) repair of the beam using SCR technique.**

The tests were carried out in a bending machine (Controls) in the architecture laboratory of the University of Guelma. The frame of this machine is equipped with a load cell of 100 kN (Figure 3). The vertical displacement was measured, in the middle section, using an LVDT sensor with a maximum stroke of 100 mm. The strains were measured using 3 strain gauges, where two are glued at the external surface of the composite bands and the third one in the tensile face in the middle of the beam (Figure 2e).



Fig 3. Machine test.

### 3. Results and discussion

#### 3.1. Global behavior

The stress/displacement curves versus the loading, of the control beam and the beam preloaded at 65% and then repaired by the GFRP composite using SCR technique are represented in Figure 4. The curves obtained show that, after the discharges (at zero loads), the presence of a permanent displacement due to inelastic behavior and therefore the existence of residual arrows which can be interpreted as an irreversibility due to the cracking of the concrete. These results are in agreement with the ones obtained by (Boussaha, 2008) and (Kreit, 2011).

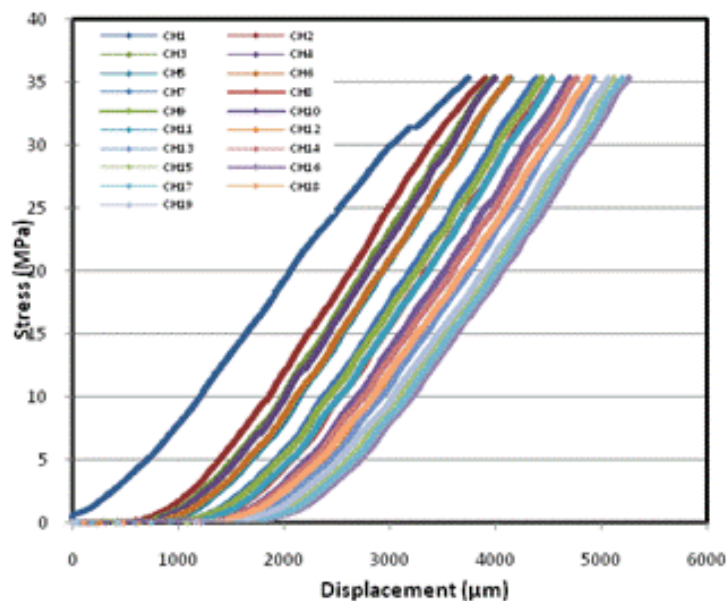


Fig 4. Stress/displacement of the beam EP\_65%\_PRFV\_E of the 19 cycles load/unload.

The analysis of Figure 5 shows that the evolution of the stress/displacement of the control beam is very close to that obtained at the first cycle (1st cycle), whereas the curve of the 19<sup>th</sup> cycle is distant from the previous one by approximately 1.64 mm (residual arrow) due to the plastification of the steel armature reinforcements of the tensile zone of the beam.

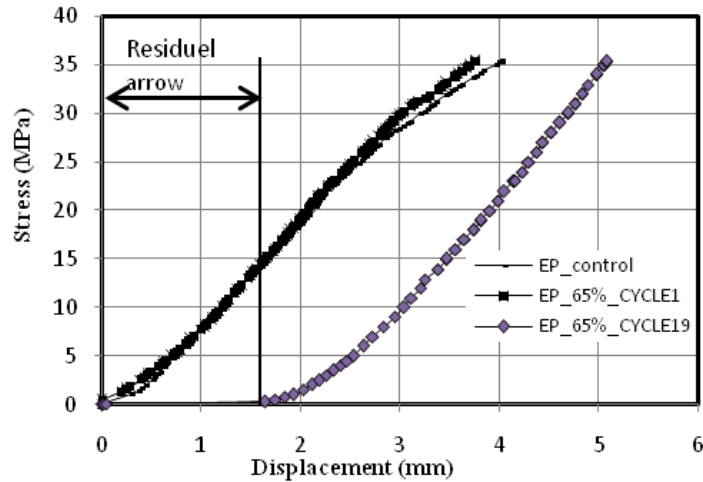


Fig 5. Evolution of the stress versus displacement of the control beam and EP\_GFRP\_65%\_Test 1 and Test 19.

The results obtained, under fatigue loading, show generally that the displacements versus the cycling (load/de-load) number of the repaired beam are higher compared to the control one. However, the maximum displacements reached during the first three cycles of the repaired beam are lower than that obtained for the control beam (Figure 6) and Table 1.

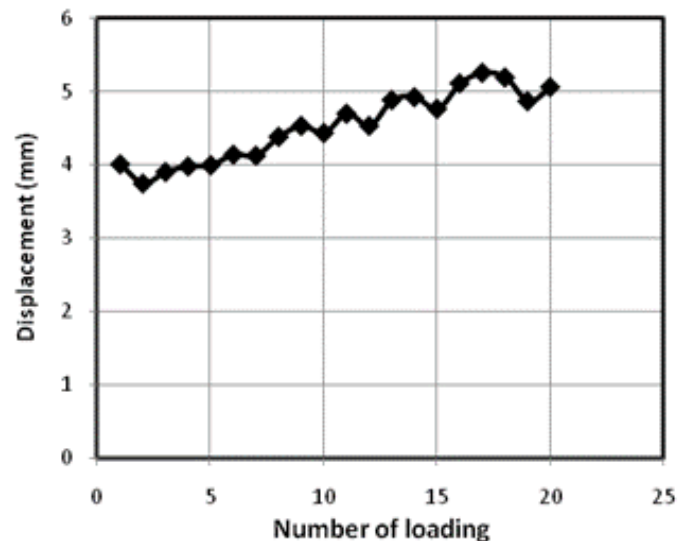


Fig 6. Evolution of the displacements versus the loading cycle numbers.

### 3.2. Influence of the repair on the stiffness of the beams

For the beam, preloaded and then repaired, bending stiffness was determined experimentally, which represents the slope of the linear part of the stress-displacement curve. The experimental results of the rigidities of the beams tested before and after the repair are presented in Figure 7.

A decrease of approximately 14.1% in the rigidity of the beam repaired with the GFRP is noticed for the 1st loading cycle compared to the control beam. However, in the second cycle, the

stiffness increased by about 17% and then slow decrease is observed while remaining greater than the rigidity of the control beam even for the 19th cycle. These results are in good agreement with the work of Shahawy and Beitelman (1999).

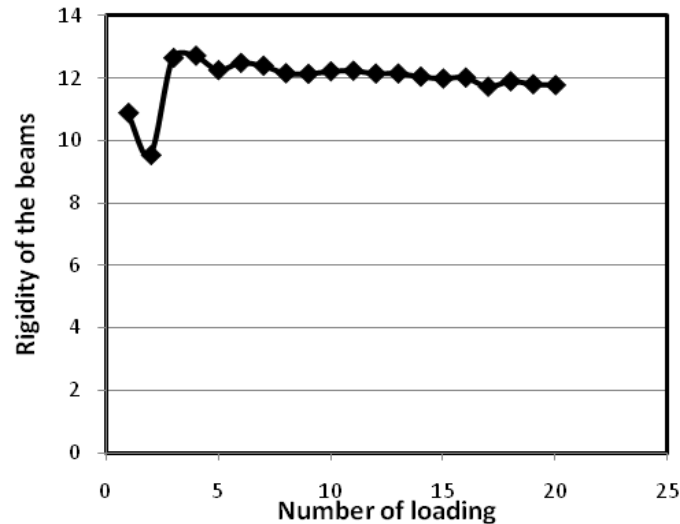


Fig 7. Stiffness of the beams during the cyclic fatigue tests.

### 3.3. Local behavior

The stress/strain curves for the first loading cycle, plotted using the strain gauges (g1, g3 and g4), which their locations are illustrated in Figure 10a, are shown in (Figures. 8 and 9). The strains are measured in the middle of the tensile zone of the concrete beam using g1, while g3 and g4 at the cracks. Table 1 recapitulates the obtained results of the strains gauges obtained by (g1, g3 and g4), displacements and rigidities of the control beam and the repaired one for the 19<sup>th</sup> tests.

Table 1. Obtained strains using strain gauges (g1, g2 and g3), displacements and rigidities of the control beam and the repaired one for the 19<sup>th</sup> tests.

N° of loading	Strains g1 ( $\mu\text{m}$ )	Strains g3 ( $\mu\text{m}$ )	Strains g4 ( $\mu\text{m}$ )	Displacements (mm)	Rigidity
Control beam	385	3566	132	4.01	10,9
Cycle 1	271	2553	2195	3.75	9,55
Cycle 2	353	2412	2742	3.91	12,66
Cycle 3	676	2303	1786	3.98	12,73
Cycle 4	736	2268	1792	4.00	12,27
Cycle 5	798	2228	1785	4.15	12,5
Cycle 6	823	2210	1802	4.13	12,41
Cycle 7	840	2156	1809	4.39	12,17
Cycle 8	865	2122	1812	4.54	12,15
Cycle 9	854	2119	1896	4.44	12,23
Cycle 10	888	---	---	4.71	12,25
Cycle 11	884	2107	1828	4.54	12,16
Cycle 12	863	2074	1813	4.89	12,16
Cycle 13	896	2092	1798	4.93	12,06
Cycle 14	891	2118	181	4.77	12
Cycle 15	893	2117	1790	5.12	12,03
Cycle 16	882	2119	1781	5.27	11,74
Cycle 17	866	2091	1784	5.2	11,91
Cycle 18	862	2134	1796	4.88	11,82
Cycle 19	864	2135	1766	5.07	11,79

Figure 8 and Table 1 show the strains increases for the strain gauge (g1) from the 3<sup>rd</sup> cycle compared to the control beam, ie an increase of 1237% for the 19<sup>th</sup> cycle.

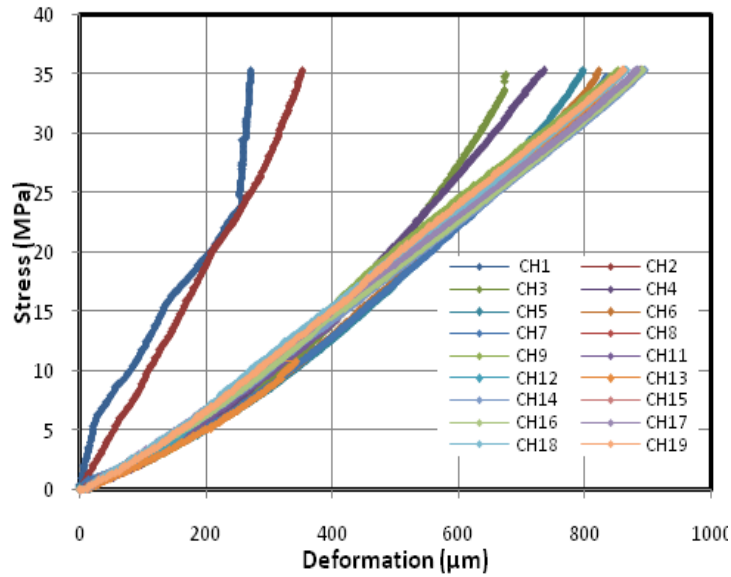


Fig 8. Stress/Strains obtained by strain gauge (g1) versus the cyclic loadings.

It should also be noted that the recorded strains of the composite with the strain gauge g3 for the repaired beam have decreased for all cycles. The strains obtained for the control beam and the repaired one after the 19<sup>th</sup> cycle are respectively 3566 and 2135 µm, i.e. a decrease of 67% is noticed. While, increases for all loadings are recorded by the strain gauge (g4), ie approximately 1238% for the 19<sup>th</sup> cycle (Figure 9, Table 1).

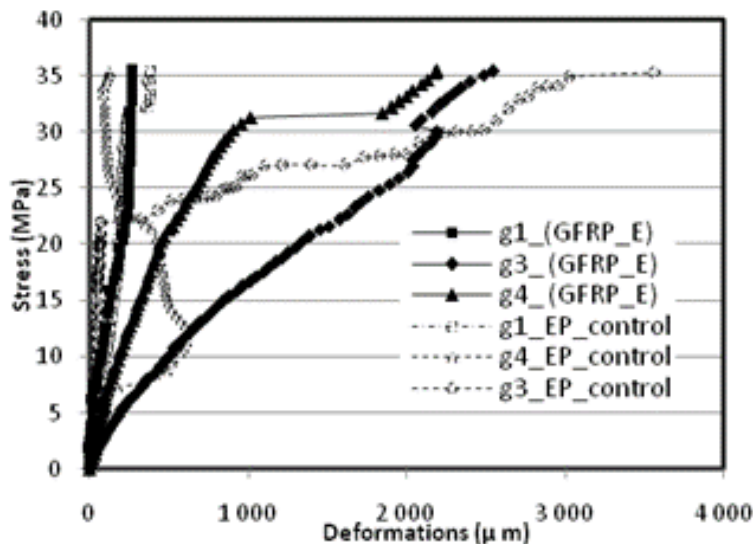


Fig 9. Stress/Strain (g1) for 1<sup>st</sup> loading cycle of the beam (GFRP\_65%\_E) and the control beam.

### 3.4 Fissuration

Figure 10a illustrates that the control beam subjected to 4-point bending has undergone a shear rupture, taking into account the type of cracking. The diagonal cracks were born on the lower supports and propagated towards the points of application of the upper load.

Whereas the beam (EP\_65%\_E) was repaired by GFRP, under a load of fatigue in the service state, the rupture was not yet reached even after 19 loadings thus showing the effectiveness of the repair adopted in this work (Figure 10b). Moreover, no peeling of the composite was detected during the tests and the beam passed the fatigue test successfully. The ductile failure mode has not been distinguished for beams repaired under fatigue loading for a service level; this will be reached in static.

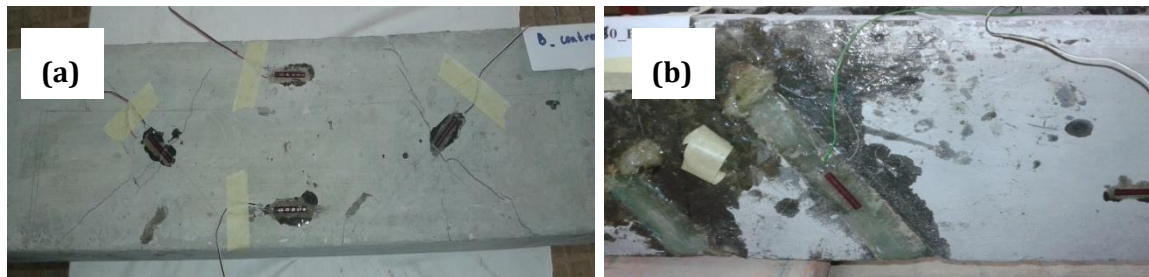


Fig 10. Failure modes

a) Control beam b) Beam preloaded at 60% then repaired by GFRP.

#### 4. Conclusions

In this study, it was shown that the repair of beams using SCR technique exhibited good fatigue behavior. The mode of failure of the repaired beam has not yet been reached even for 19<sup>th</sup> loading cycles. This result is very encouraging and must be confirmed by other tests in the future work. It is worth noticing that the presence of the composite in the shear zone not only reduced the potential crack propagation during fatigue cycles, but also stiffened the beams. Therefore, this technique has a very good resistance to fatigue loading.

#### Acknowledgments

The authors would like to acknowledge Mr BOUDJEHEM H from the Architecture laboratory of University of Guelma having to facilitate the access to the experimental machine.

#### 5. References

- Arduini, M., Nanni, A. (1997). Behavior of precracked RC beams strengthened with carbon, FRP sheets. *ASCE Journal of Composites for Construction*, 63-70.
- Barnes, R. A., Mays G. C. (1999), Fatigue performance of concrete beams strengthened with CFRP plates, *ASCE, Journal of composites for construction*, 63 – 72.
- Boumaaza, M., Bezazi, A., Bouchelaghem, H., Benzennache, N., Amziane, S. and Scarpa. F. (2017). Behavior of pre-cracked deep beams with composite materials repairs, *Techno Press, Structural Engineering and Mechanics* 61(4), 575–583.
- Boussaha, F. (2008). Comportement en fatigue des poutres en béton armé renforcées en cisaillement à l'aide de matériaux composites avancés. Thèse PhD, École de technologie supérieure, Montréal, Canada., 144.
- Choi Y. W., Lee H. K., Chu S. B., Cheong S. H, and Jung, W. Y. (2012). Shear Behavior and Performance of Deep Beams Made with Self-Compacting Concrete. *International Journal of Concrete Structures and Materials*, 6 (2), 65–78.
- De Lorenzis, L., Teng, J. G. (2007). Near-surface mounted FRP reinforcement: An emerging technique for strengthening structures. *Composites: Part B*, 38, 119–143.
- Dong, J., Wang, Q., Guan, Z. (2013). Structural behavior of RC beams with external flexural and flexural–shear strengthening by FRP sheets, *Composites: Part B*, 44, 604–612.
- Kreit, A., Mahmoud, F., Castel, A., François, A. (2011). Repairing corroded RC beam with near-surface mounted CFRP rods. *Materials and Structures* 44, 1205–1217.

- Masoud S., Soudki k., Topper T. (2001), CFRP-strengthened and corroded RC beams under monotonic and fatigue loads, *ASCE Journal of composites for construction*, pp.228 – 236.
- Meier, U., Deuring, M., Meier, H., and Schwegler, G. (1992). Strengthening of structures with CFRP laminates: Research and applications in Switzerland. *Advanced Compos. Mat. in Bridges and Struct.*, K. W. Neale and P. Labossiere, eds. Canadian Society for Civil Engineers, Montreal.
- Papakonstantinou, C. G. (2000). Fatigue performance of reinforced concrete beams strengthened with glass fiber reinforced polymer composite sheets." MS thesis, University of South Carolina, Columbia, S.C.
- Shahawy M., Beitelman T.E. (1999). Fatigue performance of RC beams strengthened with CFRP Laminates, proceedings of 1st CDDC international conference on durability of fiber reinforced polymer composite for construction, Sherbrook, August, 169-178.
- Teo, W., Hing, K.L.M., and Liew, M.S. (2017). Interaction between Internal Shear Reinforcement and External FRP Systems of RC Beams: Experimental Study. *The Open Civil Engineering Journal*, 11, 143-152.
- Wu, Z.Y. (2004). Etude expérimentale du comportement des Poutres courtes en béton armé pré-fissurées et Renforcées par matériaux composite sous Chargement statique et de fatigue. Thèse LCPC Paris, novembre.
-